
	<p>Research and Development Programme on Seismic Ground Motion</p> <p>CONFIDENTIAL  <i>Restricted to SIGMA scientific partners and members of the consortium, please do not pass around</i></p>	<p>Ref : SIGMA-2014-D2-131  Version : 01</p>
		<p>Date : October 15<sup>th</sup> 2014  Page : 1 / 3</p>



# EMPIRICAL GROUND MOTION MODEL ADAPTED TO THE FRENCH CONTEXT

AUTHORS			REVIEW			APPROVAL		
NOM	DATE	VISA	NOM	DATE	VISA	NOM	DATE	VISA
Gabriele AMERI Geoter			John DOUGLAS					
			Frank SCHERBAUM					

	<p>Research and Development Programme on Seismic Ground Motion</p> <p>CONFIDENTIAL  <i>Restricted to SIGMA scientific partners and members of the consortium, please do not pass around</i></p>	<p>Ref : SIGMA-2014-D2-131  Version : 01</p>
		<p>Date : October 15<sup>th</sup> 2014  Page : 2 / 3</p>


## Executive Summary

The objective of the SIGMA project is to improve knowledge on data, methods and tools to better quantify uncertainties in seismic hazard estimates. To this aim, 5 WPs are identified, the first three devoted to each main ingredient of the seismic hazard assessment (SHA): seismic source characterization, ground-motion characterization and site effects. The fourth WP is devoted to the development of the seismic hazard model and it is sensed to integrate all outcomes from the previous WPs into an improved seismic hazard model.

The study presented here is developed within WP 2 and it has downstream and upstream connections with the other WPs. Because the ground motion characterization is one of the key elements of any SHA and it is often identified as one of the largest contributors to the total uncertainty in the total hazard, the results of this study have direct implications on WP 4. Moreover, this study has largely benefited from the results of WP 1 and WP 3 in terms of earthquake metadata accuracy (catalogue under development in WP 1) and site characterization of French stations (WP 3). These research axes are not finalized yet and their results should be incorporated in this study in the future.

In empirical ground motion prediction equations (GMPEs) the scaling of ground motion with source properties is typically accounted by the earthquake magnitude, the style-of-faulting and, in some cases, other parameters related to the earthquake depth or to the fault geometry (e.g., dip angle). One of the most important source parameter, that is rarely accounted for in the empirical GMPEs, is the stress parameter (i.e., Brune's stress drop). Nevertheless, the stress parameter is often cited as one of the possible causes of the larger scatter of high-frequency between-event residuals for small magnitudes with respect to large magnitude events, as observed in several studies (e.g., Youngs et al., 1995; Boore et al., 2014).

The main reasons for neglecting the stress parameter in empirical GMPEs are that its estimation is typically characterized by relevant uncertainties and that the stress parameter value for future events is usually unknown and thus difficult to use in seismic hazard assessment. However, several studies have shown that differences may exist in the average values of stress parameters for different regions. This is the case, for instance, of France and Switzerland where it has been shown that stress

	<p>Research and Development Programme on Seismic Ground Motion</p> <p>CONFIDENTIAL  <i>Restricted to SIGMA scientific partners and members of the consortium, please do not pass around</i></p>	<p>Ref : SIGMA-2014-D2-131  Version : 01</p>
		<p>Date : October 15<sup>th</sup> 2014  Page : 3 / 3</p>

parameters for the French and Swiss Alps are generally lower than the ones obtained in the Rhine Graben or in the Pyrenees (Drouet et al., 2010; Edwards & Fah, 2013). This information can be accounted for in median ground-motion prediction if stress parameter scaling is included in the GMPEs.

The study detailed in this document is a follow-up of the study presented at the Scientific Committee N.6 held in Lyon on November 2013 (deliverable SIGMA-2013-D2-92, hereafter referred to as D2-92) which aimed at developing a preliminary GMPE based on RESORCE database (2013 version) including French data. The main result of D2-92 was the derivation of a GMPE that included the stress parameter in the functional form and thus allowed to account for regional differences in stress parameters for France, highlighted in the scientific literature. In this study, we continue the analyses presented in D2-92 by using essentially the same approach. With respect to D2-92 we considered the comments and suggestions made by the two reviewers and we enriched the data set by including additional data that were not considered in the first selection. A re-evaluation of metadata for French event is also performed following the release of the Si-Hex catalogue.

In light of the new data considered in this study, we carefully investigate the correlation between the between-event residuals for small magnitude events with stress parameters. With respect to D2-92, where we considered only the stress parameters provided for France by Drouet et al., (2010), in this study we also considered the stress parameters calculated for Swiss events by Edwards & Fah (2013). This allows us to strengthen the results of D2-92 showing that the between-event residuals are positively correlated with stress parameters. We include the stress parameter scaling in the functional form of the GMPEs by using the stress parameter from both studies in a consistent way. The predicted scaling is found to be in remarkably good agreement with what expected from theoretical models of the source spectrum.

This study showed that the stress parameter can be effectively included in the functional form of the GMPEs. This allows accounting for regional differences in stress parameter and, at the same time, decreasing the standard deviation of the GMPE by partially explaining the large between-event variability observed at high-frequency for small magnitude events.



**FUGRO-Group**  
**POLE GEO-ENVIRONNEMENT**  
3, rue Jean Monnet  
34 830 Clapiers - France  
**Tel:** + 33 (0)4 67 59 18 11  
**Fax:** + 33 (0)4 67 59 18 24  
**Email:** [geoter@geoter.fr](mailto:geoter@geoter.fr)  
**Website:** <http://www.geoter.fr>



## SIGMA PROJECT (WP2)

----

## EMPIRICAL GROUND MOTION MODEL ADAPTED TO THE FRENCH CONTEXT

**Document type:**

Final Report

**Identification:**

Report GTR/EDF/1014-1219

## Revisions

<b>Ind.</b>	<b>Date</b>	<b>Modifications</b>
0	15 October 2014	First emission of the Final report

<i>Client:</i> <b>EDF</b>	<i>Document type:</i> <b>Final REPORT</b>	<i>Identification:</i> GTR/EDF/1014-1219	
<i>Recipient:</i> <b>Paola TRAVERSA</b>	<i>GEOTER archive (text and figures):</i> Serveur\affaire\2012\5512	<i>Date of origin:</i> 15/10/2014	<i>Number of pages:</i> 32 p.

**REPORT TITLE:**

**SIGMA PROJECT (WP2)**

----

**EMPIRICAL GROUND MOTION MODEL ADAPTED TO  
THE FRENCH CONTEXT**

*Realization:*



**GEOTER**

Pole Geo-environnement  
3, rue Jean Monnet  
34 830 Clapiers

Tel.: 04 67 59 18 11  
Fax: 04 67 59 18 24  
Email: [geoter@geoter.fr](mailto:geoter@geoter.fr)  
Website: [www.geoter.fr](http://www.geoter.fr)

Command: n° 3000-4200447811 dated 6/12/2012

*Client approval:*

**Madame Paola TRAVERSA**  
**TEGG – Service Géologie Géotechnique**  
**905, av. du Camp de Menthe**  
**13090 Aix-en-Provence**  
**Email : [paola.traversa@edf.fr](mailto:paola.traversa@edf.fr)**  
Tel : +33 4 42 95 95 35

This document is property of the customer and must not be reproduced or communicated without its authorization

<b>Date</b>	<b>Written by</b>	<b>Reviewed by</b>	<b>Approved by</b>
15 October 2014	G. AMERI	R. SECANELL	Ch. MARTIN
<b>Visas</b>			

# TABLE OF CONTENTS

<b>1.</b>	<b>SCOPE OF THE REPORT .....</b>	<b>7</b>
<b>2.</b>	<b>DATASET .....</b>	<b>7</b>
2.1	<b>METADATA FOR FRENCH EVENTS .....</b>	<b>8</b>
2.2	<b>DATA SELECTION .....</b>	<b>10</b>
<b>3.</b>	<b>GENERAL FUNCTIONAL FORM OF THE GMPE.....</b>	<b>13</b>
<b>4.</b>	<b>RESULTS .....</b>	<b>14</b>
4.1	<b>RESIDUALS USING THE GENERAL MODEL.....</b>	<b>14</b>
4.2	<b>CORRELATION WITH STRESS PARAMETER .....</b>	<b>16</b>
4.3	<b>INCLUDING STRESS PARAMETER SCALING IN THE FUNCTIONAL FORM.....</b>	<b>19</b>
4.4	<b>DISCUSSION ON WITHIN-EVENT RESIDUALS .....</b>	<b>23</b>
4.1	<b>MAGNITUDE SCALING.....</b>	<b>25</b>
<b>5.</b>	<b>COMPARISON WITH OTHER GMPES .....</b>	<b>26</b>
<b>6.</b>	<b>CONCLUSION .....</b>	<b>29</b>
<b>7.</b>	<b>REFERENCES .....</b>	<b>31</b>

# TABLE OF ILLUSTRATIONS

Figure 1. Mw estimated by Dr10 versus Mw provided by the Si-Hex catalogue. Data are separated into Alps, Rhine-Graben and Pyrenees regions according to Dr10.....	9
Figure 2. Comparison of epicentral distances calculated using Si-Hex locations (Repi New) and RESORCE-2013 locations (Repi OLD).....	9
Figure 3: Magnitude versus distance distribution of the selected dataset. The records are color-coded according to the earthquake country. ....	11
Figure 4: Distribution of records in selected dataset in terms of site classification. Left: magnitude versus distance plot of records recorded at stations characterized by a measure of the Vs30 (gray symbol) or by an EC8 site class (red symbol). Right: magnitude versus distance distribution of records color coded according to the EC8 site class.....	12
Figure 5: Histogram of the Vs30 values associated to the records in the selected dataset. ....	12
Figure 6: Number of earthquakes (left) and records (right) as a function of period for the selected dataset compared to those selected in D2-92. ....	13
Figure 7: between-event residuals as a function of Mw (top) and within-event residuals as a function of epicentral distance (bottom) for PGA (left column) and T=1s (right column). The mean and standard deviation of the residuals calculated for different distance bins are shown by blue bars.....	15
Figure 8: between-event residuals versus Mw for PGA (left) and PSA at 1 s (right). The residuals are color-coded according to the event country.....	15
Figure 9: PGA (T=0s) between-event residuals versus stress parameters for different regions, classified as reported by Dr10 and EF13. The dashed line show the PGA scaling with stress parameter with respect to a reference value at 140 bars predicted by AB06 for a Mw=4. ....	17
Figure 10: PGA (T=0s) between-event residuals versus stress parameters for common events in the EF13 and Dr10 studies. ....	18
Figure 11: The same as Figure 9 but the between-event residuals are for PSA at 1 second. ....	19
Figure 12: differences between logarithms of stress parameter values by Dr10 and by EF13 for common events in the two datasets plotted versus Mw as provided by Dr10. ....	20
Figure 13: Between-event residuals for PGA (left column) and T=1s (right column) as a function of Mw. In the upper plots, blue bars show the mean and standard deviation calculated for different magnitude bins. In the lower plots the residuals are colored according to the earthquake country.....	21
Figure 14: Between-event, within-event and total standard deviations (from bottom to top) including or not equation 6 in the functional form.....	21
Figure 15: log <sub>10</sub> PSA scaling factors predicted for a factor of 4, 2 and 0.5 difference with respect to the reference stress parameters by this study and by Atkinson & Boore (2006) for Mw=4. ....	22
Figure 16: Scaling of acceleration response spectra with stress parameter for France for a Mw=4.5 at 20 km.....	23
Figure 17: Within-event residuals for PGA (left column) and T=1s (right column) as a function of epicentral distance. First line: all residuals, mean and standard deviation calculated for different distance bins are shown by blue bars. Second line: yellow symbols show residuals for French records, mean and standard deviation calculated for different distance bins are shown by black bars. Third line: black symbols show residuals for French Alps records, mean and standard deviation calculated for different distance bins are shown by black bars. Fourth line: green symbols show residuals for Pyrenees records, mean and standard deviation calculated for different distance bins are shown by black bars.....	24
Figure 18: Within-event residuals for PGA versus kappa values by Dr10. Black crosses show residuals for each record. Black dots show station residuals (average of within-event residuals for on station) for the French Alps region. Green dots show station residuals for the Pyrenees region. Yellow dots show station residuals for the Rhine Graben region.....	25
Figure 19: Magnitude scaling for PGA (left) and spectral acceleration at T=1s (right). Red symbols are ground motions corrected for distance (at 10 km), site, style-of-faulting, stress parameter and averaged for each event. The blue line represents the model magnitude scaling.....	26
Figure 20: Magnitude scaling of PGA estimated at a distance of 20 km. Rupture distance for the Faccioli10 GMPEs is calculated using conversion equations by Scherbaum et al., (2004). ....	27



Figure 21: Magnitude scaling of PSA at T=1s estimated at a distance of 20 km. A rupture distance of 23km is used for Faccioli10 GMPE. Rupture distance for the Faccioli10 GMPEs is calculated using conversion equations by Scherbaum et al., (2004). .....27

Figure 22: Distance scaling of PGA estimated for a Mw=6. Rupture distance for the Faccioli10 GMPEs is calculated using conversion equations by Scherbaum et al., (2004). .....28

Figure 23: Distance scaling of PSA at T=1s estimated for a Mw=6. Rupture distance for the Faccioli10 GMPEs is calculated using conversion equations by Scherbaum et al., (2004). .....28

Figure 24: Total standard deviation (sigma) for the GMPEs considered in this section for comparison (see text for explanation). For the BSSA14 model, the sigma is computed for a Mw=6 and Rjb=20 km. ....29

# PROJET SIGMA (WP2)

----

## EMPIRICAL GROUND MOTION MODEL ADAPTED TO THE FRENCH CONTEXT

---

### 1. SCOPE OF THE REPORT

---

The study detailed in this document is a follow-up of the study presented at the Scientific Committee N.6 held in Lyon on November 2013 (deliverable SIGMA-2013-D2-92, hereafter referred to as D2-92) which aimed at developing a preliminary GMPE based on RESORCE database (2013 version) including French data. The main result of D2-92 was the derivation of a GMPE that included the stress parameter in the functional form and thus allowed to account for regional differences in stress parameters for France, highlighted in the scientific literature. In this study, we continue the analyses presented in D2-92 by using essentially the same approach. With respect to D2-92 we considered the comments and suggestions made by the two reviewers and we enriched the data set by including additional data that were not considered in the first selection. A re-evaluation of metadata for French events is also performed following the release of the Si-Hex catalogue.

In light of the new data considered in this study, we carefully investigate the correlation between the between-event residuals for small magnitude events with stress parameters. With respect to D2-92, where we considered only the stress parameters provided for France by Drouet et al., (2010), in this study we also considered the stress parameters calculated for Swiss events by Edwards & Fah (2013). This allows us to strengthen the results of D2-92 showing that the between-event residuals are positively correlated with stress parameters. We include the stress parameter scaling in the functional form of the GMPEs by using the stress parameter from both studies in a consistent way. The predicted scaling is found to be in remarkably good agreement with what expected from theoretical models of the source spectrum.

---

### 2. DATASET

---

The dataset used in this study is extracted from the RESORCE-2013 database (SIGMA-2013-D2-91) which is an updated version of the RESORCE database (SIGMA-2011-D2-15; Akkar et al., 2014). The database is composed by strong-motion records recorded in the broader European and Middle Eastern area with a maximum magnitude given by the 1999 Kocaeli earthquake,  $M_w=7.6$  (if we exclude the singly recorded event of 1969 off the coast of Portugal with  $M_w=7.8$ ). With respect to the previous version, RESORCE-2013 is enriched with a number of data from small-to-moderate magnitude earthquakes, mainly from France, Switzerland and Greece.

RESORCE-2013 has been already described and discussed in details in previous SIGMA deliverables (SIGMA-2013-D2-92) and in scientific publications and we will not further detail the database compilation methodology here. However, in the next section, we will discuss the metadata of French events being of special relevance for the SIGMA project and for the purpose of this study.

The Swiss events included in RESORCE are characterized by  $M_w$  provided, for almost all of them, by the time-domain moment-tensor inversion performed by the Swiss Seismological Survey (<http://www.seismo.ethz.ch/prod/tensors>). For this reason, these events are also characterized by a reliable fault mechanism.

## 2.1 METADATA FOR FRENCH EVENTS

For a large number of French earthquakes (about 80%) the  $M_w$  is not provided in RESORCE-2013. The magnitude of these events is given in terms of local magnitude ( $M_L$ ) as provided by RéNaSS (<http://renass.unistra.fr/>). Moreover, for many of these events, the style-of-faulting is not known, which further limits the use of these data for deriving GMPEs. In D2-92, we used the  $M_w$  estimated by spectral inversion by Drouet et al. (2010), hereafter referred to as Dr10, if available; otherwise  $M_L$ - $M_w$  conversion equations proposed by the Dr10 were used.

After the compilation of D2-92, the Si-Hex catalogue Version 2 has been released (<http://www.franceseisme.fr/sismicite.html>). This catalogue represents the most updated source of information on the metadata of event occurred in metropolitan France. In particular, the  $M_w$  are estimated using a homogeneous procedure for the French territory based on coda wave magnitude for  $M_w > 3.4$  and on a newly calibrated  $M_{LDG}$ - $M_w$  conversion equation for  $M_w < 3.4$ . Moreover, the provided hypocentral locations are the most precise available among the sources of information compiled within the Si-Hex project and, if available, regional velocity models are used to relocate the events.

In Figure 1, we compared the  $M_w$  values derived by Dr10 with the ones provided in Si-Hex. The events are separated according to Alps, Rhine-Graben and Pyrenees regions. There is a slight tendency to have larger  $M_w$  values in Dr10 with respect to Si-Hex for the bulk of the data, particularly evident for the Pyrenees region. It is hard to comment on the origin of the differences between Dr10 and Si-Hex magnitude estimations as no uncertainties are reported in the studies. Further comments on this aspect will be provided later in this deliverable.

Figure 2 shows a comparison between source-to-site epicentral distances calculated using Si-Hex and RESORCE-2013 locations. It is interesting to note that the differences in epicentral distances may be quite significant and their impact may be important especially at short epicentral distances where the data are scarce.

In this study, we decided to update the epicentral locations of the French events reported in RESORCE-2013 with the values provided by Si-Hex. In terms of  $M_w$ , we continue preferring the values provided by spectral inversion by Dr10, if available, and for the other events we used the Si-Hex  $M_w$  values.

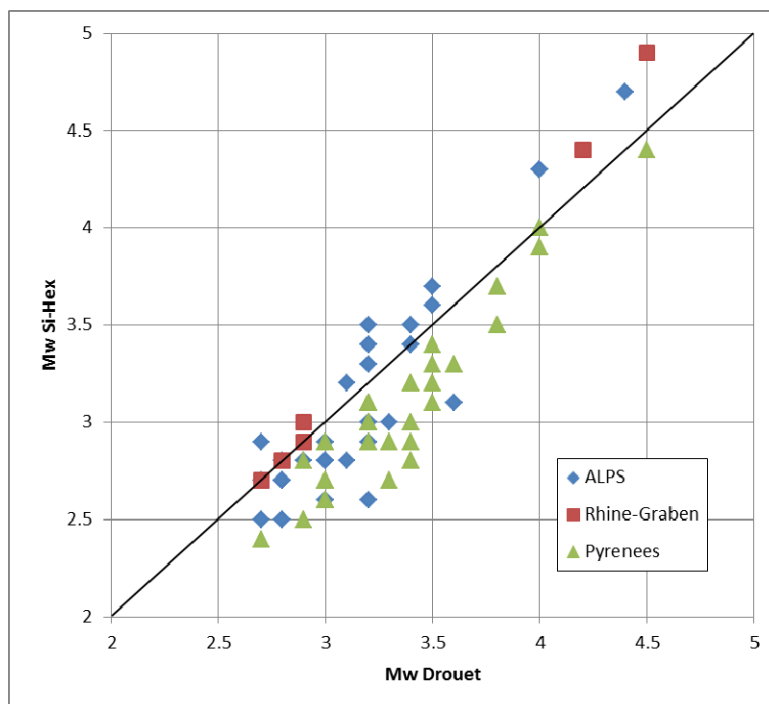


Figure 1. Mw estimated by Dr10 versus Mw provided by the Si-Hex catalogue. Data are separated into Alps, Rhine-Graben and Pyrenees regions according to Dr10.

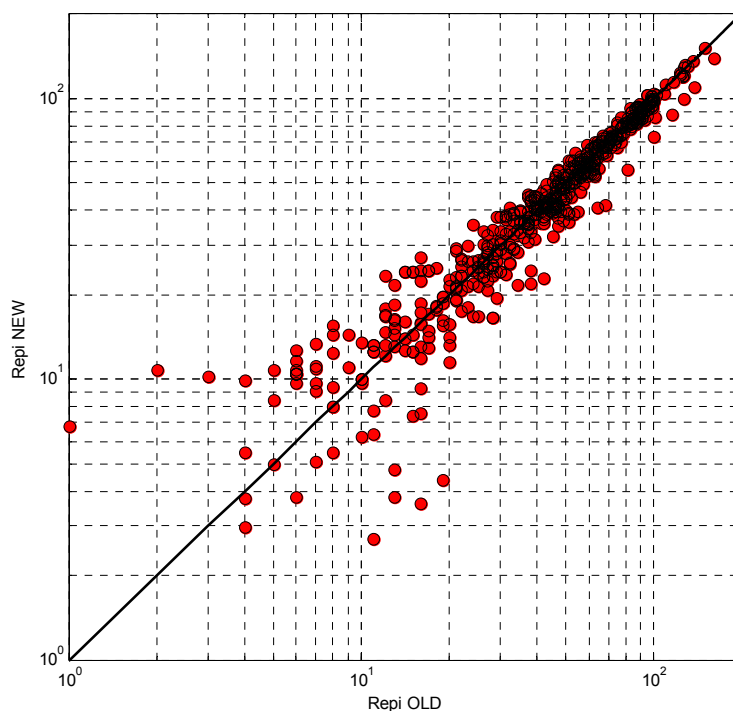


Figure 2. Comparison of epicentral distances calculated using Si-Hex locations (Repi New) and RESORCE-2013 locations (Repi OLD).

As already discussed in D2-92, the style-of-faulting is missing for 94 events in RESORCE-2013 (excluding singly-recorded event). A bibliographic research was conducted in order to identify studies devoted to the analysis of seismic

sequence and where information on fault mechanism of small events could be retrieved. Table 1 summarizes the papers providing the style-of-faulting information for 15 French events.

Table 1. Events for which the dominant style of faulting is defined in this study based on bibliographic research.

Event Date (yyyymmdd hhmm)	Style-of-faulting	Reference paper
19990111 0336	Strike-slip	Thouvenot et al. 2003
19991101 1722	Strike-slip	Courboulexet al. 2007
20001219 1420	Strike-slip	Courboulexet al. 2007
20001220 0545	Strike-slip	Courboulexet al. 2007
20020905 2042	Normal	Rigo et al. 2005
20021211 2009	Normal	Rigo et al. 2005
20040718 0216	Normal	Cara et al. 2007
20061024 0004	Normal	Sylvander et al. 2008
20061117 1819	Normal	Sylvander et al. 2008
20061118 2034	Normal	Sylvander et al. 2008
20061118 2217	Normal	Sylvander et al. 2008
20061119 1316	Normal	Sylvander et al. 2008
20061120 0401	Normal	Sylvander et al. 2008
20061216 0817	Normal	Sylvander et al. 2008
20071115 1347	Normal	Sylvander et al. 2008

For the remaining events, the fault mechanism was estimated based on the dominant stress regime and the seismotectonic zonation developed at France national level by Baize et al. (2013). We are aware that this is a quite rough approach but we believe that it gives a first order approximation on the dominant fault mechanism of the event.

## 2.2 DATA SELECTION

A selection is made on the RESORCE-2013 database in order to remove a number of data that we considered not usable, not relevant for the aim of the study or not relevant for seismic hazard studies in active crustal regions. The data selection is very similar to the one applied in D2-92. The following exclusion criteria are employed:

- events with depth larger 30 km;
- records with epicentral distances > 200 km;
- Mw smaller than 3;
- stations that are known to be not in free field (e.g., located in galleries or in dams);
- records that have not been processed or for which only one horizontal component is available;
- Stations that are not characterized by either Vs30 or EC8 site class information (i.e., stations with no reported information of the site characteristics).
- Turkish and Italian events for which only converted Mw are available. These events are identified by a flag in RESORCE-2013 and as shown in D2-92 they inflate the between-event variability of the residuals likely due to poor accuracy of the Mw.
- Singly-recorded events
- Records filtered with low-pass corner frequency  $\leq 20\text{Hz}$  and, for each period  $T$ , recordings filtered with high-pass corner frequency  $f_{hp} \geq 1/(1.25 T)$ .

With respect to the data selection performed in D2-92 the two major differences are:

- 1) We considered all the records up to 200 km down to  $M_w=3$ . In D2-92 the magnitude-distance filter applied in REOSORCE-2013 was retained. Here, we preferred to have a more homogeneous distribution of data for small magnitudes in order to comment on possible trend of residuals with distance.
- 2) Based on the comments of one the reviewer of D2-92 we included the stations for which a value of  $V_{s30}$  is provided in RESORCE-2013, but the method used and the origin source of such value are classified as “unknown”. These are about 150 stations with metadata from ESD or ISESD.
- 3) In the dataset selected for D2-92 there was an error in the metadata table containing  $V_{s30}$  values and a number of French stations (about 10) was not considered.

The records distribution as a function of magnitude and epicentral distance obtained after the application of the exclusion criteria is shown in Figure 3, where the records are color-coded on a country base. The events with magnitude larger than 4 are mostly Italian and Turkish with a smaller contribution of Greek earthquakes. Considering smaller magnitudes (Figure 3, right) the dataset is largely composed by Swiss and French events. The selected dataset contains about 380 events and 2350 records. In the final dataset there are 433 records from 65 French events and 109 records from 22 Swiss events.

The site conditions of the recording stations in RESORCE-2013 is characterized by the  $V_{s30}$  (the time-averaged shear-wave velocity of the top 30m), where available, and alternatively by a EC8 site class estimated according to different studies and methodologies (Akkar et al.,2013a). As already pointed out in D2-92,  $V_{s30}$  is not available for a large number of the stations in RESORCE-2013. Moreover, the number of station with  $V_{s30}$  became almost irrelevant when considering French and Swiss data. This is a specific subject of investigation within the WP3 where  $V_{s30}$  measurements are ongoing for a number of French stations and they will provide important information for the improvement of the site model in the present study.

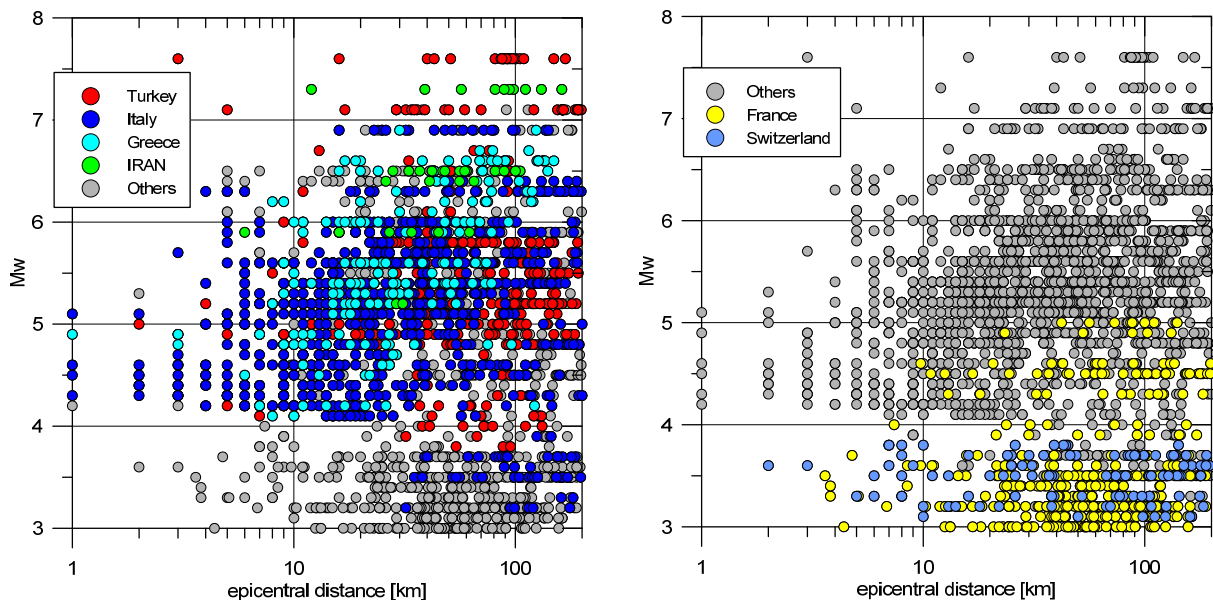


Figure 3: Magnitude versus distance distribution of the selected dataset. The records are color-coded according to the earthquake country.

Figure 4 shows the distribution of records in terms of site classification of the recording station. Roughly 40% of the records are associated to a  $V_{s30}$  value, 50% to an EC8 site class and about 10% lack of information on the station site condition. Figure 5 shows the histograms of the  $V_{s30}$  values available in the selected dataset.

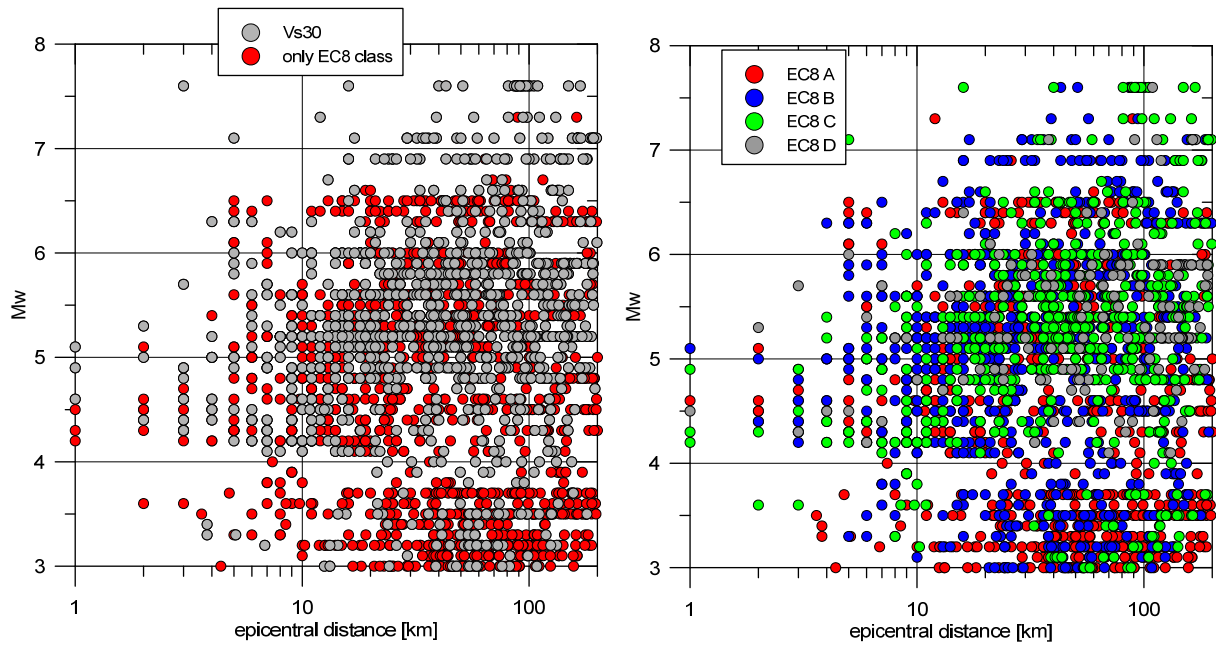


Figure 4: Distribution of records in selected dataset in terms of site classification. Left: magnitude versus distance plot of records recorded at stations characterized by a measure of the Vs30 (gray symbol) or by an EC8 site class (red symbol). Right: magnitude versus distance distribution of records color coded according to the EC8 site class.

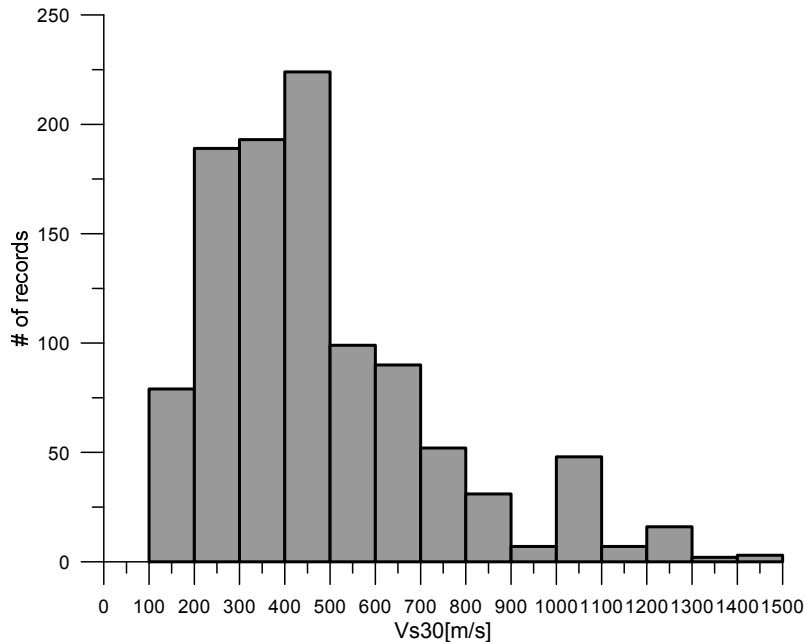


Figure 5: Histogram of the Vs30 values associated to the records in the selected dataset.

As mentioned above, the dataset is not uniform for different spectral periods because of the exclusion criteria on the usable frequency band. The number of usable earthquakes and records as a function of spectral period is shown in Figure 6, where the dramatic decrease of number of data is visible starting at about 1s. For this reason, as also done in D2-92, we considered spectral ordinates up to 3 seconds.

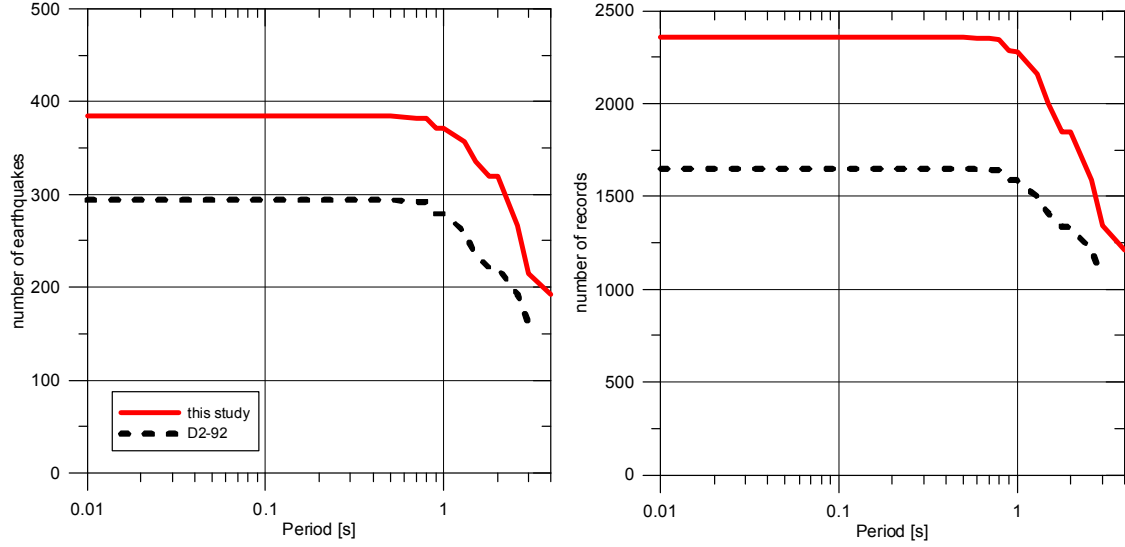


Figure 6: Number of earthquakes (left) and records (right) as a function of period for the selected dataset compared to those selected in D2-92.

### 3. GENERAL FUNCTIONAL FORM OF THE GMPE

The functional form is the same as the one proposed in D2-92 and based on previous studies (e.g. Boore and Atkinson, 2008; Akkar and Bommer, 2010; Bindi et al. 2013):

$$\log_{10} Y = a + F_D(R, M) + F_M(M) + F_S + F_{sof} \quad (1)$$

where the distance ( $F_D$ ) and the magnitude ( $F_M$ ) functions are given by:

$$F_D(R, M) = \left[ c_1 + c_2 (M - M_{ref}) \right] \log_{10} \left( \sqrt{R^2 + h^2} / R_{ref} \right) \quad (2)$$

$$F_M(M) = \begin{cases} b_1 (M - M_h) + b_2 (M - M_h)^2 & \text{for } M \leq M_h \\ b_3 (M - M_h) & \text{otherwise} \end{cases} \quad (3)$$

The functional form for  $F_D$  includes a magnitude-dependent geometrical spreading term. A term describing the logarithmic decay with distance of the of ground motion, that typically accounts for anelastic attenuation, is not included because it was found not statistically different from zero in the range of distances considered in this study (0-200 km). A further discussion on this topic will be presented later in the document. Following D2-92 and as suggested by Bommer and Akkar (2012), the regressions are performed considering both a point-source and an extended-source measure of the source-to-site distance  $R$ , namely the Joyner and Boore distance  $R_{JB}$  and the epicentral distance  $R_{EPI}$ . The results in this document will be presented in terms of  $R_{EPI}$ .

The functional form for  $F_M$  includes a linear and a quadratic scaling for magnitudes lower than  $M_h$  and only a linear scaling for larger magnitudes. Based on analysis of event-terms versus magnitude (event-specific records corrected



for distance, site and style-of-faulting) results, the variables  $M_{ref}$ ,  $M_h$ ,  $R_{ref}$  (equations 2 and 3) have been fixed to 5.5, 6.75 and 1km, respectively. Coefficient  $b_3$  was constrained to be non-negative, in first trial regressions, and subsequently, as it was found not statistically different from zero, it was constrained to zero. The functional form for the magnitude scaling will be discussed more in detail later.

The term  $F_{sof}$  in equation (1) represents the style-of-faulting correction and it is given by  $F_{sof} = f_j E_j$ , for  $j=1, \dots, 3$ , where  $f_j$  are the coefficients to be determined during the analysis and  $E_j$  are dummy variables used to denote the different fault-mechanism classes: normal (N), reverse (R), strike-slip (S). The reference style of faulting condition (i.e. parameter constrained to zero in the regressions) is class S.

The term  $F_S$  in equation (1) represents the site amplification. As extensively discussed in D2-92, we opted for a site model based on EC8 site classes in order to be able to include in the dataset a sufficient number of French data. We showed that using the EC8 class characterization of the sites is equivalent to using a Vs30 characterization, with respect to the uncertainty. In equation (1) we used:

$$F_S = s_1 F_A + s_2 F_B + s_3 F_C + s_4 F_D \quad (4)$$

where  $s_j$  ( $j=1, \dots, 4$ ) are the coefficients to be determined through the regression analysis, while  $F_A$ ,  $F_B$ ,  $F_C$ ,  $F_D$  are dummy variables that takes the values of 0 or 1 according to the four considered EC8 site classes (A to D). The regression for the EC8 model is performed constraining to zero the coefficient for class A (reference site class).

As response variable  $Y$  we used, the geometric mean of the horizontal components for peak ground acceleration (PGA in  $\text{cm/s}^2$ ) and with 5% damped pseudo-spectral acceleration (PSA in  $\text{cm/s}^2$ ) computed over 27 periods in the range 0.01-3 s. The regressions are performed applying a random effect approach (Abrahamson and Youngs, 1992), that allows to determine the components of the standard deviation of the regression (commonly referred to as sigma,  $\sigma$ ), namely the between-events ( $\tau$ ) and the within-event ( $\phi$ ) components. The total sigma is thus:

$$\sigma = \sqrt{\tau^2 + \phi^2} \quad (5)$$

Additional explanatory variables related to the source model (e.g. hanging/foot walls effect; depth to the top of the rupture; etc.) or other measure for the source-to-station distance (e.g. distance from the rupture) are not considered because of the lack of information in RESORCE-2013.

---

## 4. RESULTS

---

### 4.1 RESIDUALS USING THE GENERAL MODEL

The performance of the general function form described in the previous section is evaluated by analysis of between-event and within-event residuals versus the considered explanatory variable. Figure 7 shows the between-event and within-event residuals plotted versus Mw and epicentral distance, respectively. The residuals from the general GMPE are well behaved and no clear trends are visible as a function of magnitude or distance. However, the PGA between-event residuals show a remarkably larger variability for small magnitude events with respect to longer periods residuals. On the other hand the variability for larger magnitude is quite similar. Figure 8 shows the between-event residuals color-coded according to the earthquake country. As already observed in D2-92 the large variability of the residuals at small magnitude is due to French and Swiss events which present a larger scatter with respect to larger magnitudes. In the next section, we attempt to explain such variability as related to the variability of stress parameter of French and Swiss earthquakes.

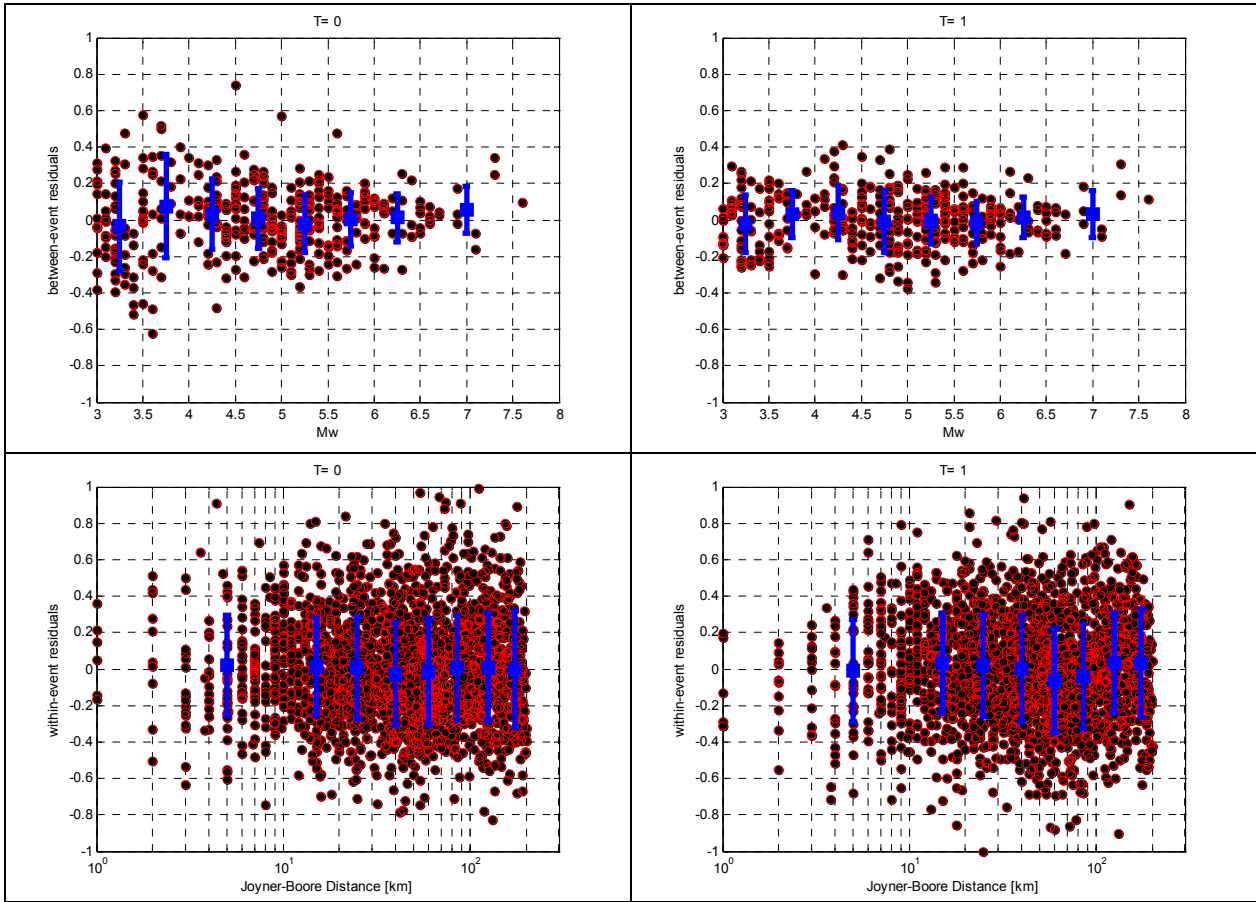


Figure 7: between-event residuals as a function of Mw (top) and within-event residuals as a function of epicentral distance (bottom) for PGA (left column) and T=1s (right column). The mean and standard deviation of the residuals calculated for different distance bins are shown by blue bars.

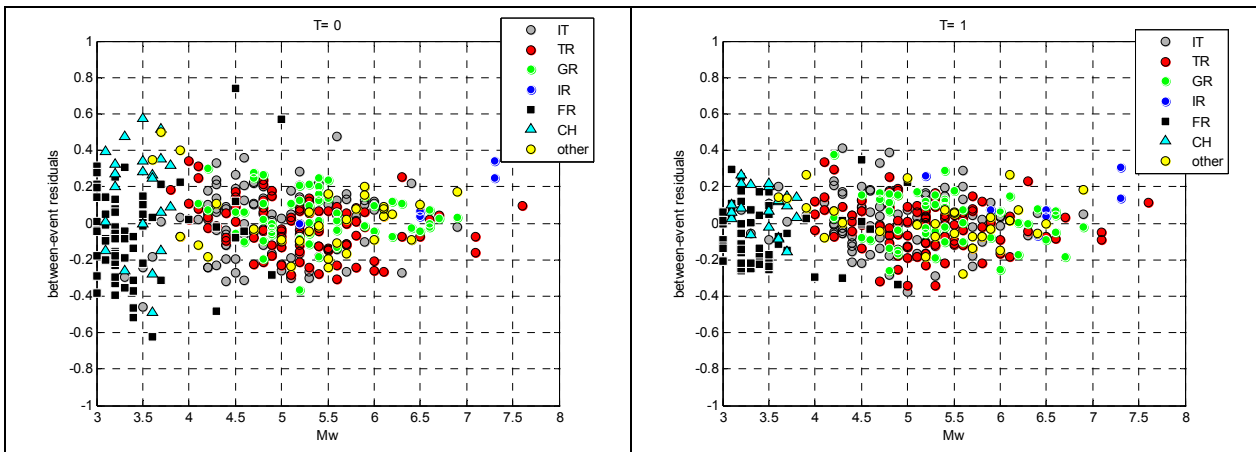


Figure 8: between-event residuals versus Mw for PGA (left) and PSA at 1 s (right). The residuals are color-coded according to the event country.

## 4.2 CORRELATION WITH STRESS PARAMETER

As done in D2-92, we try to correlate the between-event residuals with stress parameters available in literature for the region of interest in the SIGMA project. The reason for this is that several studies pointed out that there may be regional differences in the average stress parameter associated to small-to-moderate magnitude events (Dr10, EF13). On one hand, we attempt to include in the functional form the scaling of ground motion with stress parameter in order to use information from available studies to capture regional ground motion variability. On the other hand, by including the dependence on stress parameter we aim to partially reduce the aleatory variability of the model.

We considered two studies providing indication of regional differences in stress parameters for the area of interest: Dr10 and Edwards and Fah (2013), hereafter EF13. The results by Dr10 were already considered in D2-92 whereas results by EF13 were not taken into account but their use was identified as interesting for the continuation of the study. We recall here that Dr10, performed a parametric inversion in order to separate source, path and site effects from the Fourier spectra of the recordings from a large number of earthquakes in France and found different average stress values for events in the French Alps, in the Pyrenees and in the Rhine Graben. In particular events in the French Alps are on average characterized by smaller stress drop with respect to events in the other two regions, where the stress drop is found to be similar (though slightly larger in the Pyrenees). The study by EF13 applied a similar approach to Swiss events, differentiating into stress parameters in the Swiss Alps and in the Swiss Foreland. The stress parameters in the Swiss foreland are found to be on average larger than in the Swiss Alps. These two studies use different datasets and slightly different methodology but share a number of common events that are considered in both datasets.

The stress parameter by Dr10 is calculated as (Brune, 1970):

$$\Delta\sigma = \frac{7}{16} Mo \left( \frac{fc}{0.37\beta} \right) \quad (6),$$

where the corner frequency ( $fc$ ) for each event is provided in Dr10, the seismic moment ( $Mo$ ) is available in the database and the shear-wave velocity  $\beta=3.5$  km/s. For EF13 the stress parameters are directly provided by the Authors and are based on the same model with identical value of  $\beta$ . Figure 9 shows the residuals versus stress parameters in the different regions provided by Dr10 and EF13. Figure 9 also shows the scaling of PGA with stress parameter (with respect to a reference stress of 140 bars) as derived by stochastic simulations by Atkinson and Boore (2006) for a  $Mw=4$  event (this magnitude has been selected because comparable of that of the considered events). This latter serves as a reference in order to show the scaling that we would expect theoretically assuming an omega-square point-source model. Note that, what it is important is the slope of the line and not the position along the x-axis, which is due to the reference stress adopted by AB06 (the line would have the same slope considering smaller reference stress parameters).

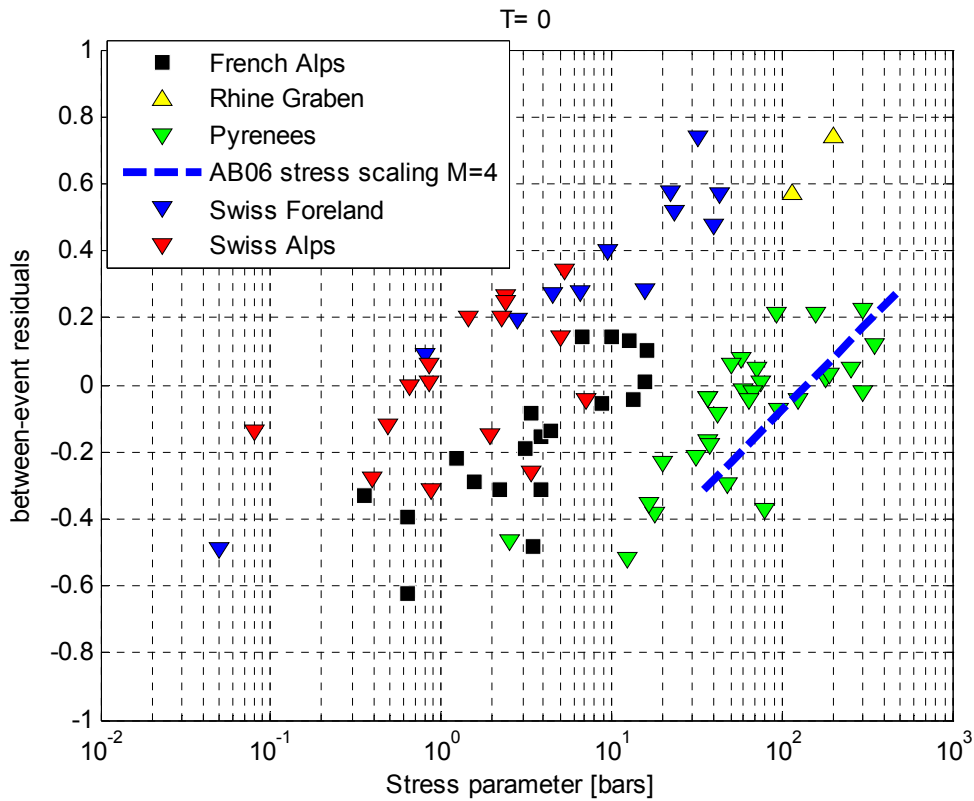


Figure 9: PGA ( $T=0s$ ) between-event residuals versus stress parameters for different regions, classified as reported by Dr10 and EF13. The dashed line show the PGA scaling with stress parameter with respect to a reference value at 140 bars predicted by AB06 for a  $M_w=4$ .

Figure 9 shows some interesting results as well as some unclear points:

1. There is a positive correlation of between-events residuals with stress parameter at short periods within the different regions.
2. The slope of the correlation is similar across different regions and consistent with scaling from Atkinson & Boore (2006) based on the omega-square source model;
3. Stress parameters for Swiss events are, on average, smaller than those of French events. This is also shown in Figure 10 where we plot the between-event residuals versus stress parameter only for common events in EF13 and Dr10 datasets. Indeed the stress parameters derived in the two studies are not directly comparable in term of absolute values and caution must be used when mixing them because the accelerometric records employed are different and because the method adopted by the authors consider different assumptions. In particular, the difference in the calculated stress parameters can be explained in terms of differences in the attenuation model considered in the two studies (Goertz-Allmann and Edwards, 2014). Essentially EF13 used a constant Q model with quite large Q values whereas Dr10 used a frequency-dependent Q with stronger attenuation and hence required that the source radiated more energy (higher stress-parameters).
4. The residuals from Pyrenees events show an unexpected behavior. Their position in Figure 9 suggests that Pyrenees data provide almost the same between-event residuals as the French Alps events although the first are characterized by a stress parameter which is, on average, the double. This is clearly in contrast with what we would expect in terms of scaling of ground motion with stress parameter. We do not have a final explanation to this result at the moment but we think that this distribution of the residuals for Pyrenees is

related to the larger Mw values estimated by Dr10 with respect to the Si-Hex ones, for Mw < 4, highlighted in Figure 1. We may suppose, for example, that Dr10 Mw estimates for Pyrenees are biased high, due to a too weak attenuation (due to the trade-off of Mw with attenuation parameters in the inversion, see also Drouet et al., 2008). The use of smaller Mw (for example the Si-Hex ones) would produce between-event residuals that would be shifted towards larger values in Figure 9. Moreover, a bias in the Dr10 Mw for Pyrenees would imply that the corner frequencies and stress parameters are biased too and should be recalculated. In case the bias concerns the geometrical spreading term, a correction of the spectra for a stronger geometrical spreading may have no effect on the corner frequencies (because the source spectra would be simply shifted down) but would lead to a reduction of the stress parameters.

Figure 11 shows the between-event residuals for spectral acceleration at 1 second versus stress parameter as done in Figure 9 for PGA. The correlation of residuals with stress parameter is much weaker with respect to what observed for PGA. Anyway, if we exclude the Pyrenees data, some correlation is still visible in the data from French and Swiss Alps, with a slope which is again consistent with the predictions from the stochastic model of Atkinson & Boore (2006). Finally, Figure 11 shows that Pyrenees events are all characterized by negative residuals supporting the fact that Mw of Pyrenees events estimated by Dr10 may be biased towards larger values.

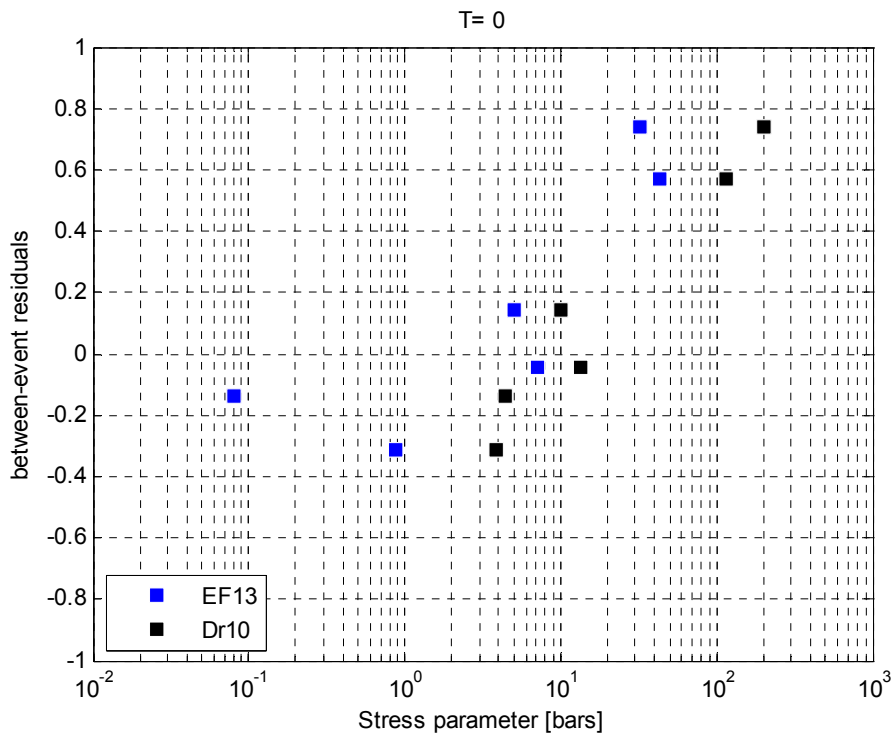


Figure 10: PGA (T=0s) between-event residuals versus stress parameters for common events in the EF13 and Dr10 studies.

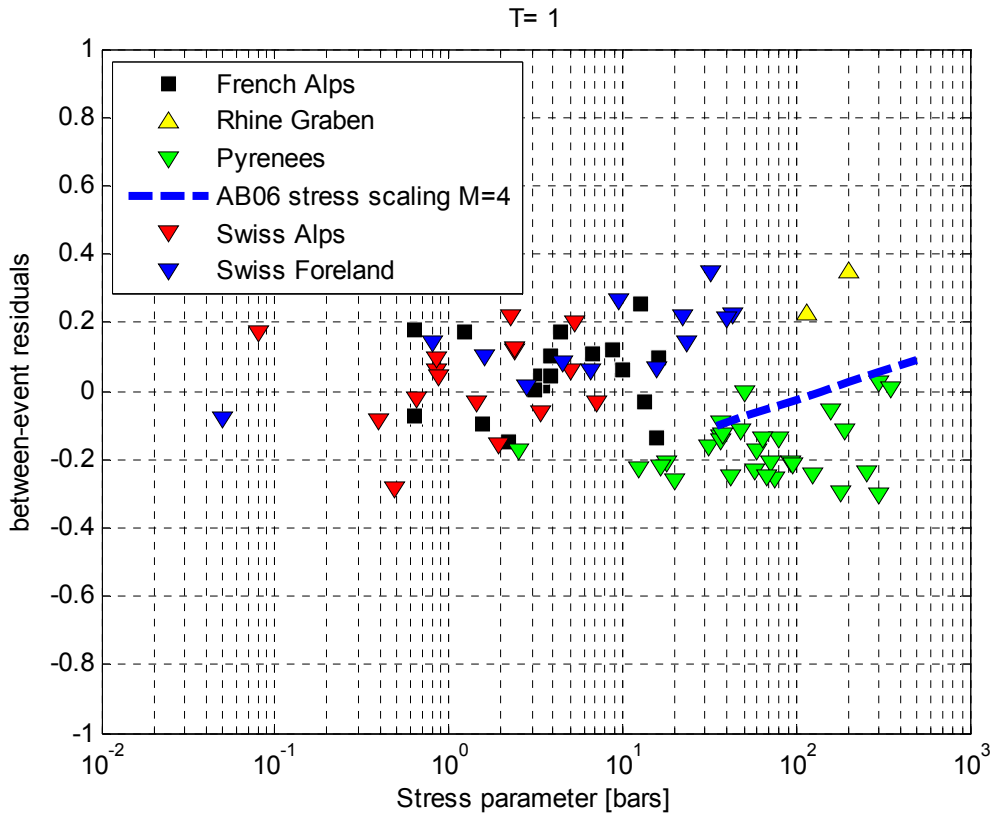


Figure 11: The same as Figure 9 but the between-event residuals are for PSA at 1 second.

### 4.3 INCLUDING STRESS PARAMETER SCALING IN THE FUNCTIONAL FORM

We attempt to include the scaling of ground motion with stress parameter in the functional form of the GMPE taking into account all the considerations we have done in the previous section. In particular, on the one hand we want to capture the scaling of ground motion with stress parameter that, as we have seen in Figure 9, is similar over the different regions. On the other hand, we want to use both values by Dr10 and EF13 although, as we have seen, these values are not consistent. Finally, we have the problem of Pyrenees data for which we have doubts on the validity of Mw and stress parameter values, but where, the scaling of residuals with stress parameters is visible and consistent with other regions.

As done in D2-92 and as suggested by Figure 9 we model the scaling of ground motion with stress parameter by a simple function of the log of the stress parameter as follows:

$$F_{stress}(\Delta\sigma) = r_1 \log_{10} \left( \frac{\Delta\sigma}{\Delta\sigma_{REF}} \right) \quad (7)$$

where  $r_1$  is the coefficient to be determined in the regression and  $\Delta\sigma_{REF}$  is a reference stress parameter value. In order to use consistently the stress values provided by Dr10 and EF13 we corrected these latter values by a scaling factor derived from the average difference of stress values for common events in the two datasets. Figure 12 show the differences of the log of stress parameters for the common events in Dr10 and EF13 datasets. Note that we considered all the common events and not only the events contained in RESORCE-2013. The mean log difference is 0.66 that correspond to a factor of 4.55. Thus, the stress parameters for Swiss events provided by EF3 were multiplied by 4.55 in order to derive equation 7.

In equation 7, we use  $\Delta\sigma_{REF} = 20$  bars which is the mean of log values of stress parameters for the French and Swiss data.

Concerning the Pyrenees events, we decided to do not include them in the calculation of the stress parameter model. We believe that these data should be used only after that the Mw and stress parameters have been verified and possibly recalculated, if necessary.

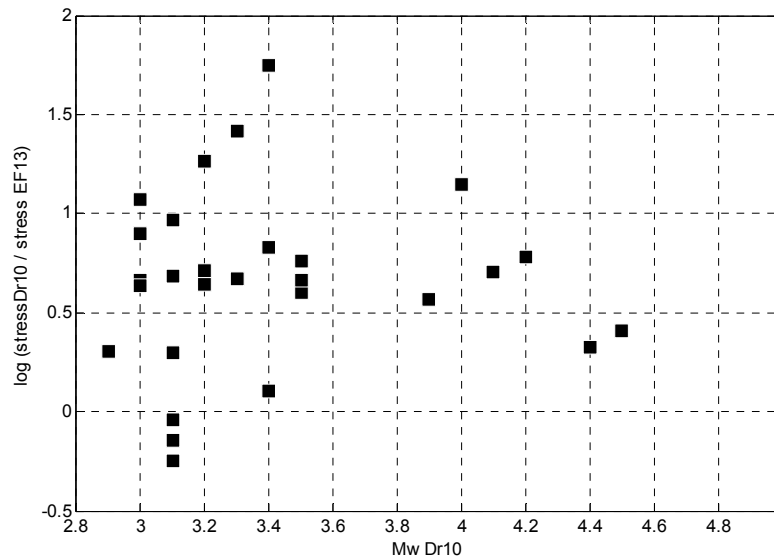
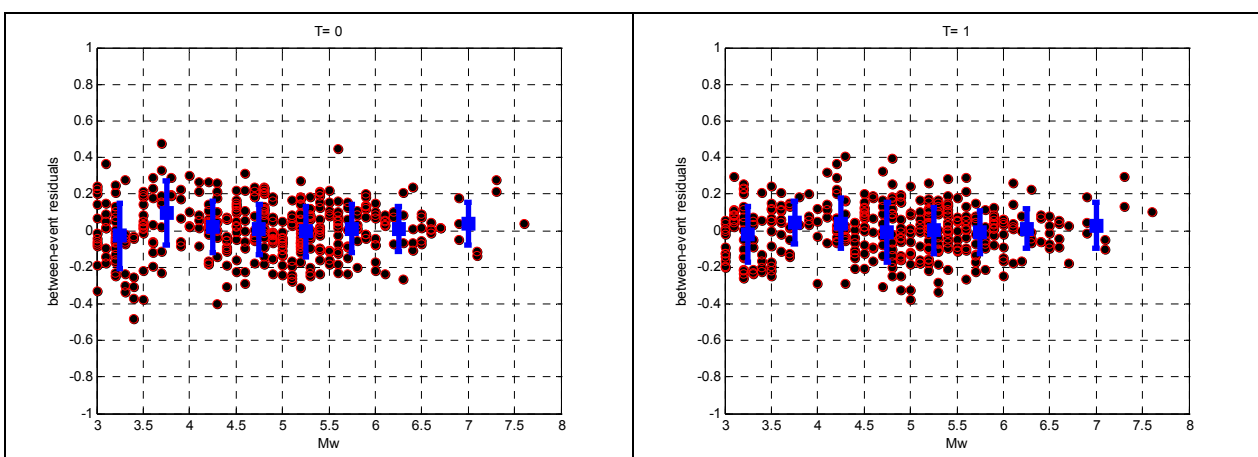


Figure 12: differences between logarithms of stress parameter values by Dr10 and by EF13 for common events in the two datasets plotted versus Mw as provided by Dr10.

If we consider equation 7 in the regression model we obtain the between-event residuals as presented in Figure 13. As we can see the residuals for PGA now show a much smaller scatter which is comparable which the one for larger magnitudes.



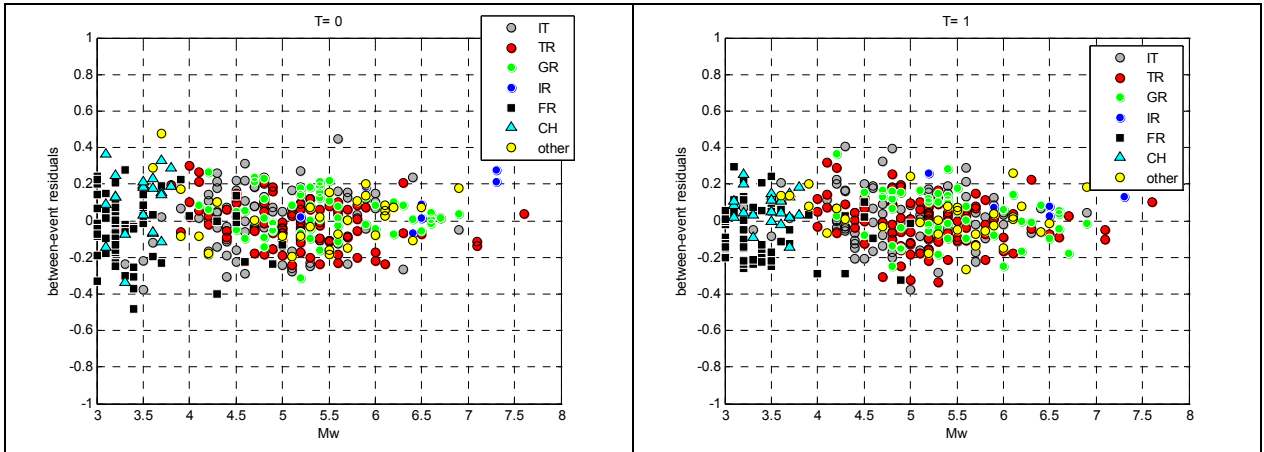


Figure 13: Between-event residuals for PGA (left column) and T=1s (right column) as a function of Mw. In the upper plots, blue bars show the mean and standard deviation calculated for different magnitude bins. In the lower plots the residuals are colored according to the earthquake country.

Figure 14 shows the reduction in the between-event and total standard deviation of the GMPE by including the stress parameter scaling as modeled in equation 6. We observe a reduction of the between-event variability at short periods, whereas, as expected the within-event variability is unaffected.

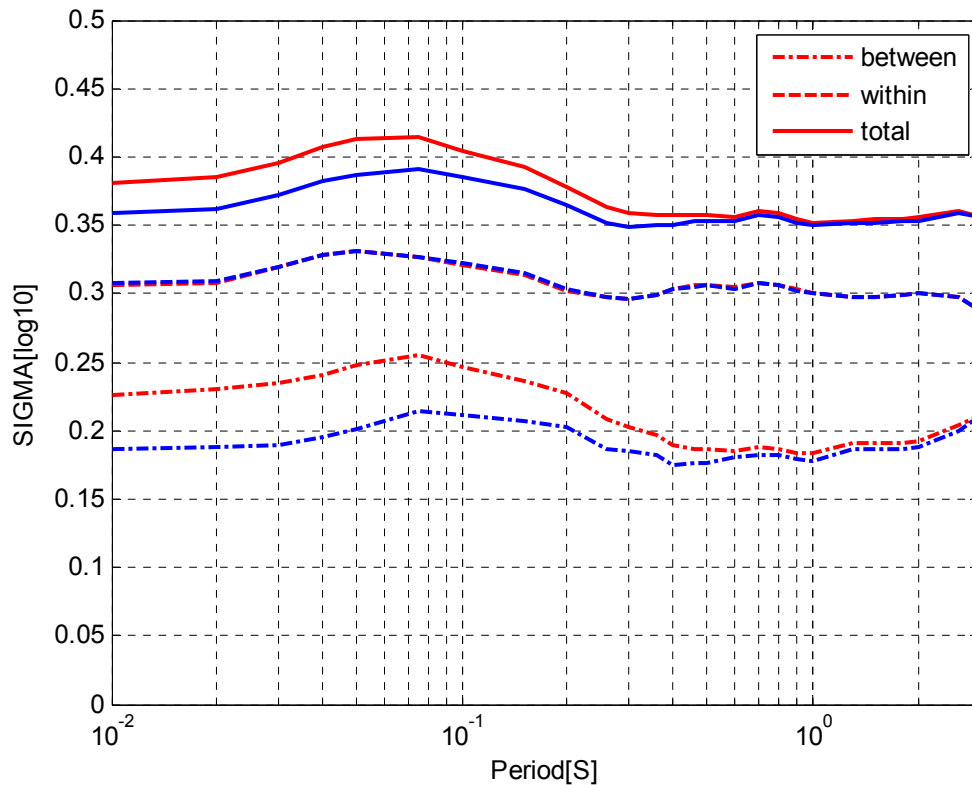


Figure 14: Between-event, within-event and total standard deviations (from bottom to top) including or not equation 6 in the functional form.

Figure 15 shows the spectral acceleration scaling for factors predicted by the model for variations of a factor of 2, 4 and 0.5 with respect of the reference stress parameter. The predicted factor are compared to those of Atkinson & Boore (2006) for a Mw=4. We note that there is a remarkable agreement between what derived empirically in this study for French and Swiss events and what predicted by the omega-square model for similar magnitudes. This



suggests that the variability of between-event residual depicted in Figure 9 can be ascribed almost completely to stress parameter scaling.

Finally, Figure 16 illustrate the scaling of the predicted response spectra with stress parameter, for a Mw=4.5 event at 20 km. The model predicts increasing ground motion for stress parameters larger than the reference stress (20 bars) and decreasing ground motion for stress smaller than the reference value.

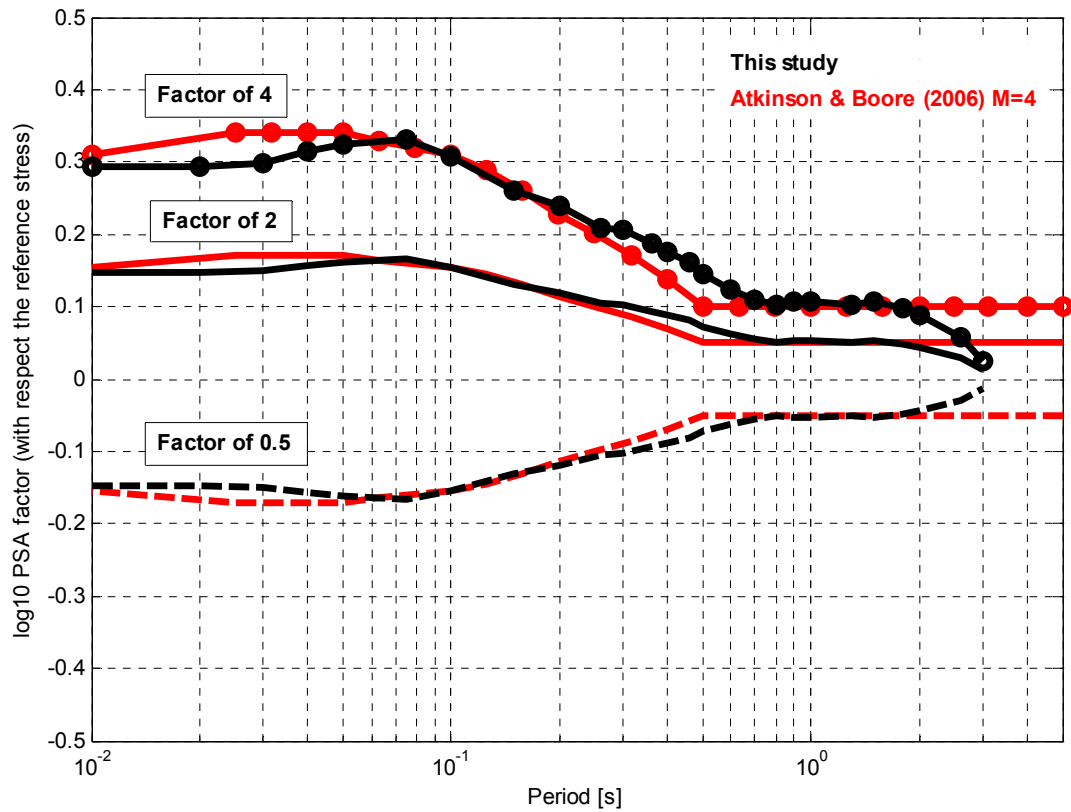


Figure 15:  $\log_{10}$  PSA scaling factors predicted for a factor of 4, 2 and 0.5 difference with respect to the reference stress parameters by this study and by Atkinson & Boore (2006) for Mw=4.

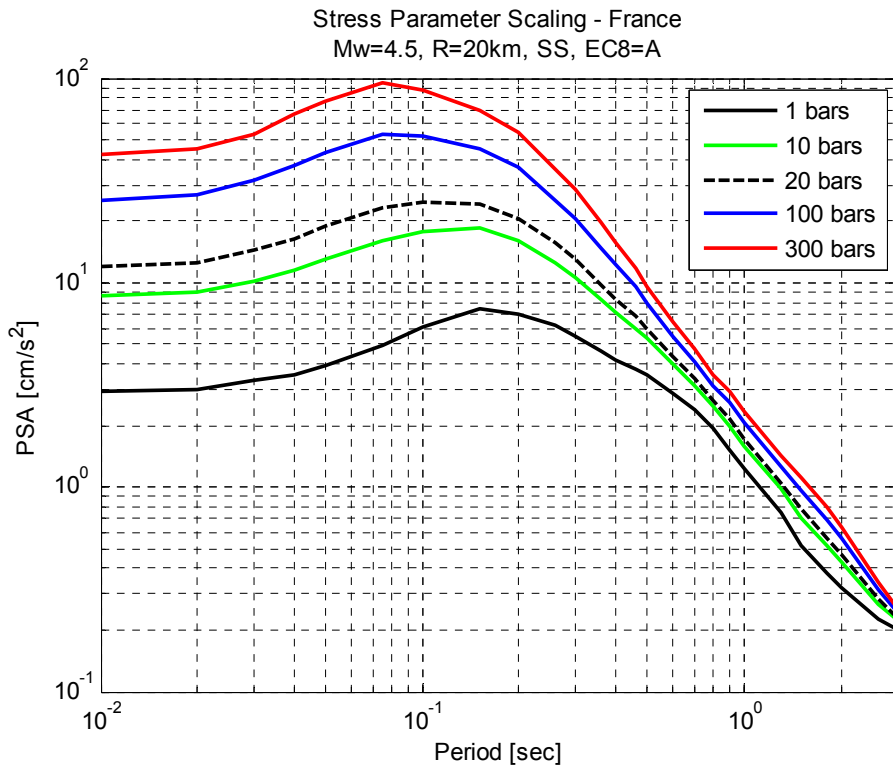


Figure 16: Scaling of acceleration response spectra with stress parameter for France for a Mw=4.5 at 20 km.

#### 4.4 DISCUSSION ON WITHIN-EVENT RESIDUALS

In this section we analyze the within-event residuals as a function of distance for specific subset of data in order to investigate possible regional trends. Figure 17 presents the within-event residuals for PGA and 1 second spectral acceleration where the mean and standard deviation of the residuals over distance bins are show by the vertical bars. Figure 17a shows the residuals for the whole dataset. Figure 17b shows the residuals for French records. Figure 17c shows the residuals for the French Alps regions and Figure 17c shows the residuals for the Pyrenees regions. No apparent trend is visible in the within-event residuals, at least in Figure 17a and Figure 17b where the data are enough to highlight possible trends. Considering French Alps and the Pyrenees, the number of data is not large enough to provide clear results , but in any case, we do not see any systematic trend.

One of the reviewers of D2-92 pointed out that there may be a dependency of the high-frequency within-event residuals on kappa values. In Figure 18, we plot the within-event residuals versus kappa values as derived by Dr10 from high-frequency slope of response-spectra site-amplification functions for more than 60 French stations. The within-event residuals are also averaged for each station in order to represent the station residuals versus the station kappa values. From Figure 18 we do not observe any clear correlation between kappa values and station residuals, although of course, the number of data is quite limited.

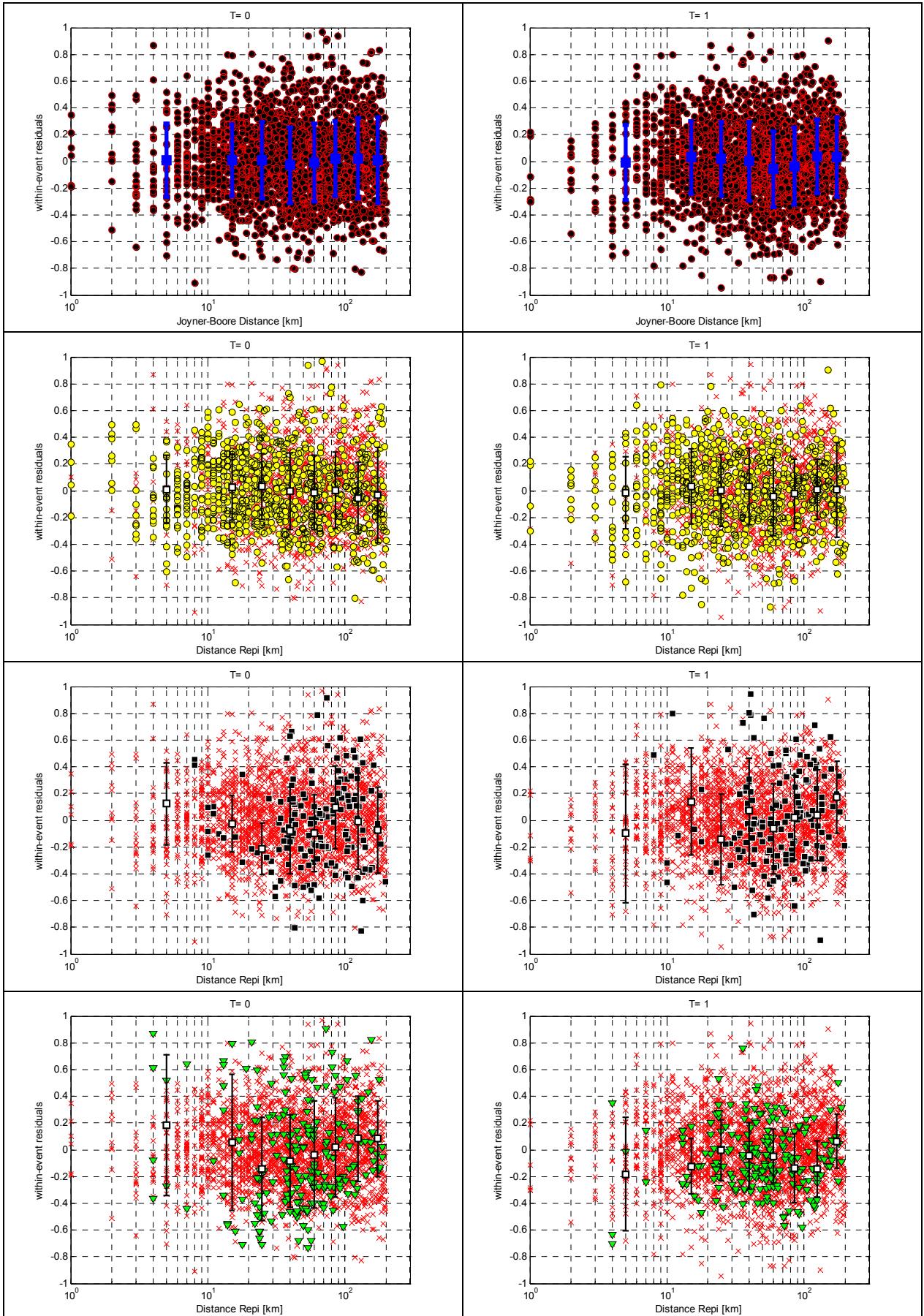


Figure 17: Within-event residuals for PGA (left column) and T=1s (right column) as a function of epicentral distance. First line: all residuals, mean and standard deviation calculated for different distance bins are shown by blue bars. Second line: yellow symbols

show residuals for French records, mean and standard deviation calculated for different distance bins are shown by black bars. Third line: black symbols show residuals for French Alps records, mean and standard deviation calculated for different distance bins are shown by black bars. Fourth line: green symbols show residuals for Pyrenees records, mean and standard deviation calculated for different distance bins are shown by black bars

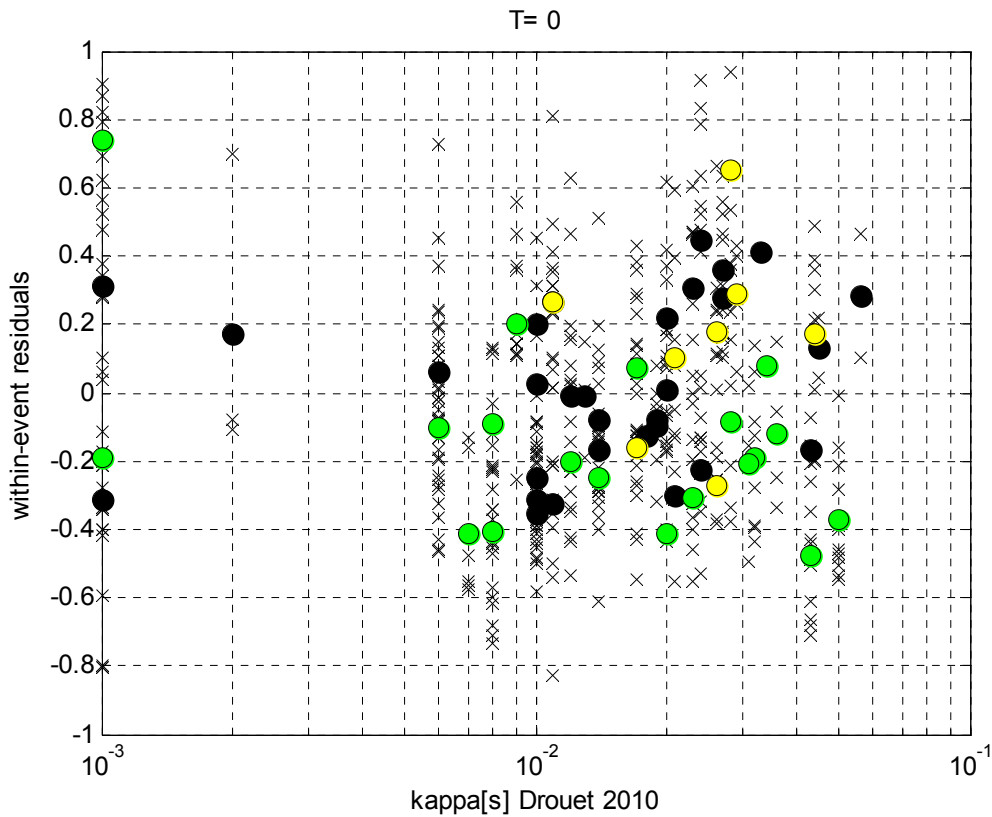


Figure 18: Within-event residuals for PGA versus kappa values by Dr10. Black crosses show residuals for each record. Black dots show station residuals (average of within-event residuals for on station) for the French Alps region. Green dots show station residuals for the Pyrenees region. Yellow dots show station residuals for the Rhine Graben region.

## 4.1 MAGNITUDE SCALING

The functional form for the magnitude scaling (equation 3) was selected based on previous studies and on the inspection of several plots similar to those reported in Figure 19. These plots show the spectral accelerations (at different periods) corrected for distance (at a reference distance of 10 km), style-of-faulting, site class, stress parameter and averaged for each event. In this way, we highlight only the magnitude dependence of the corrected spectral accelerations. Figure 19 shows that the selected functional form is able to adequately model the observed magnitude scaling over the whole range of magnitudes considered in this study. Unfortunately the number of earthquakes with  $M_w > 6.5$  is scarce and the magnitude scaling for such larger magnitudes need to be considered poorly constrained. As pointed out by Akkar et al. (2014), the RESORCE data at large magnitude basically provide the same fit to a quadratic, cubic and quadratic-hinged magnitude scaling. This currently represents a relevant source of epistemic uncertainties in the development of GMPEs using European data.

Finally, we point out that no magnitude oversaturation is observed in the present dataset.

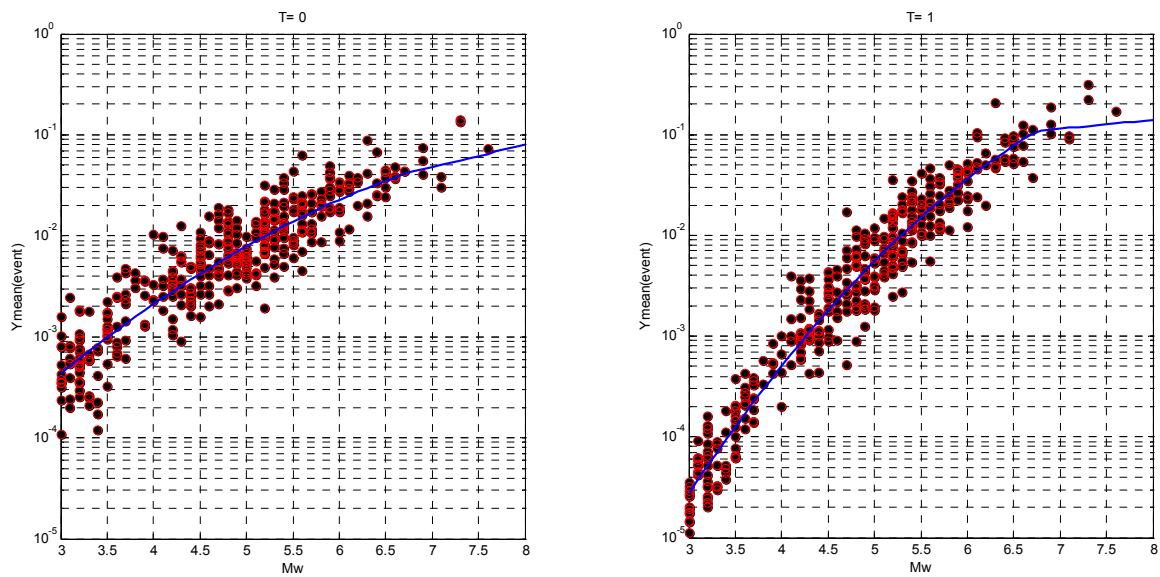


Figure 19: Magnitude scaling for PGA (left) and spectral acceleration at T=1s (right). Red symbols are ground motions corrected for distance (at 10 km), site, style-of-faulting, stress parameter and averaged for each event. The blue line represents the model magnitude scaling.

---

## 5. COMPARISON WITH OTHER GMPEs

---

In this section, we present a brief comparison of the derived GMPE with the one previously proposed in D2-92 and with other models available in recent literature. In the following comparisons, the stress parameter model is not considered in equation 1.

Figure 20 and Figure 21 show a comparison of magnitude scaling of spectral ordinates at 20 km for PGA and PSA at T=1 s, respectively. The magnitude scaling obtained in this study is compared to Boore et al., (2014) [BSSA14], Faccioli et al., (2010) and Bindi et al., (2014) as well as with the results of D2-92. The magnitude scaling is quite consistent among the different models, except for BSSA14 where the use of a hinge Mw of 5.5 for PGA represents a major difference with respect to the other GMPEs. BSSA14 predicts larger PGA for moderate magnitudes (5.5 – 6.0) with respect to the other models.

Figure 22 and Figure 23 show a comparison of distance scaling for a Mw=6 event for PGA and PSA at T=1s, respectively. Also for distance scaling the different model provide consistent results, which the exception of the BSSA14 model that provides larger PGA at all distances.

Finally , Figure 24 compares the total standard deviation of the considered GMPEs. The sigma values of the model developed in this study are comparable with other non-NGA GMPEs.

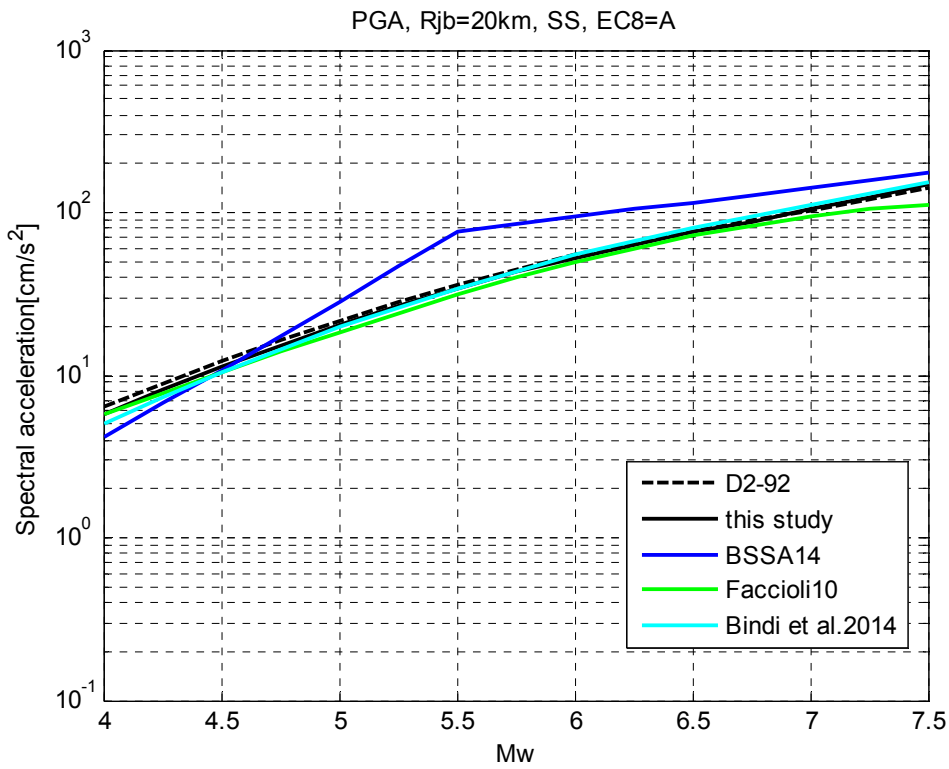


Figure 20: Magnitude scaling of PGA estimated at a distance of 20 km. Rupture distance for the Faccioli10 GMPEs is calculated using conversion equations by Scherbaum et al., (2004).

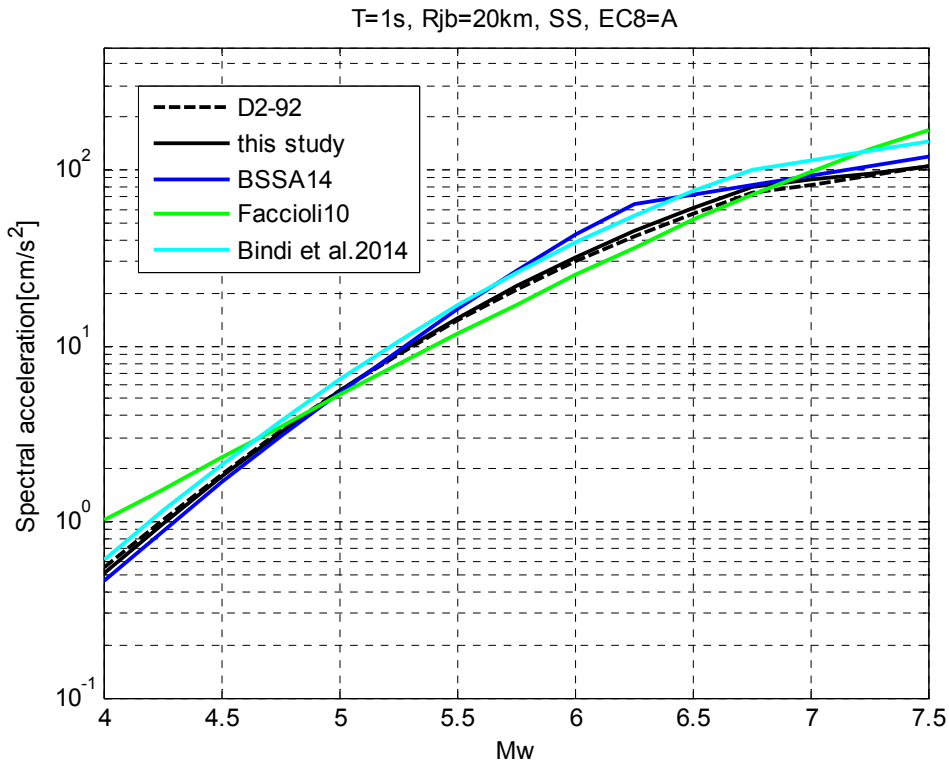


Figure 21: Magnitude scaling of PSA at T=1s estimated at a distance of 20 km. A rupture distance of 23km is used for Faccioli10 GMPE. Rupture distance for the Faccioli10 GMPEs is calculated using conversion equations by Scherbaum et al., (2004).

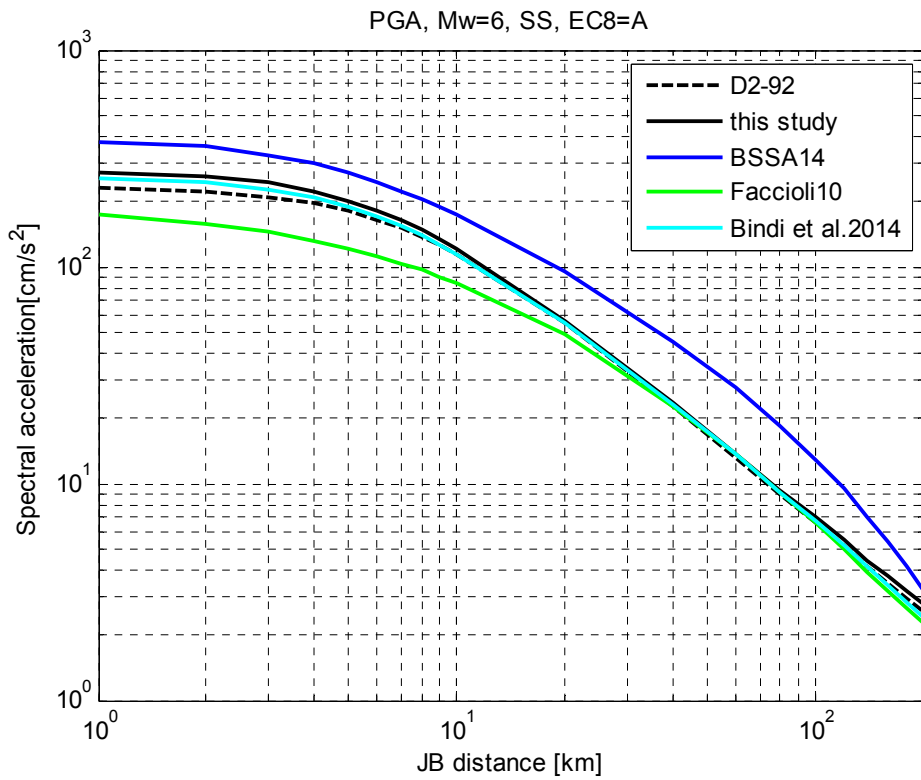


Figure 22: Distance scaling of PGA estimated for a Mw=6. Rupture distance for the Faccioli10 GMPEs is calculated using conversion equations by Scherbaum et al., (2004).

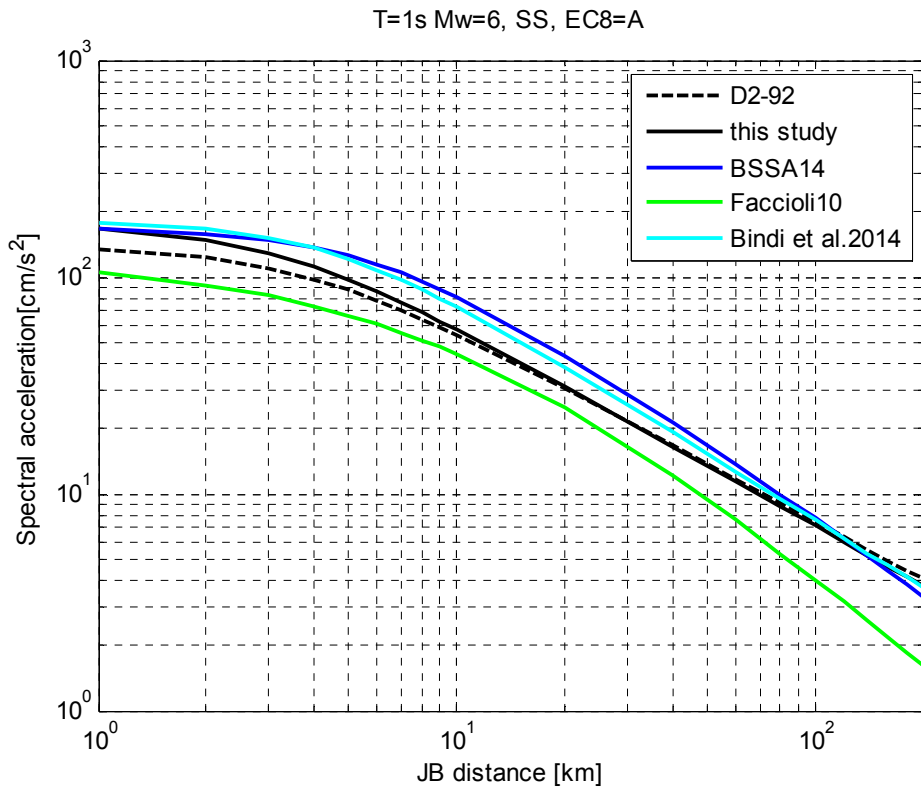


Figure 23: Distance scaling of PSA at T=1s estimated for a Mw=6. Rupture distance for the Faccioli10 GMPEs is calculated using conversion equations by Scherbaum et al., (2004).

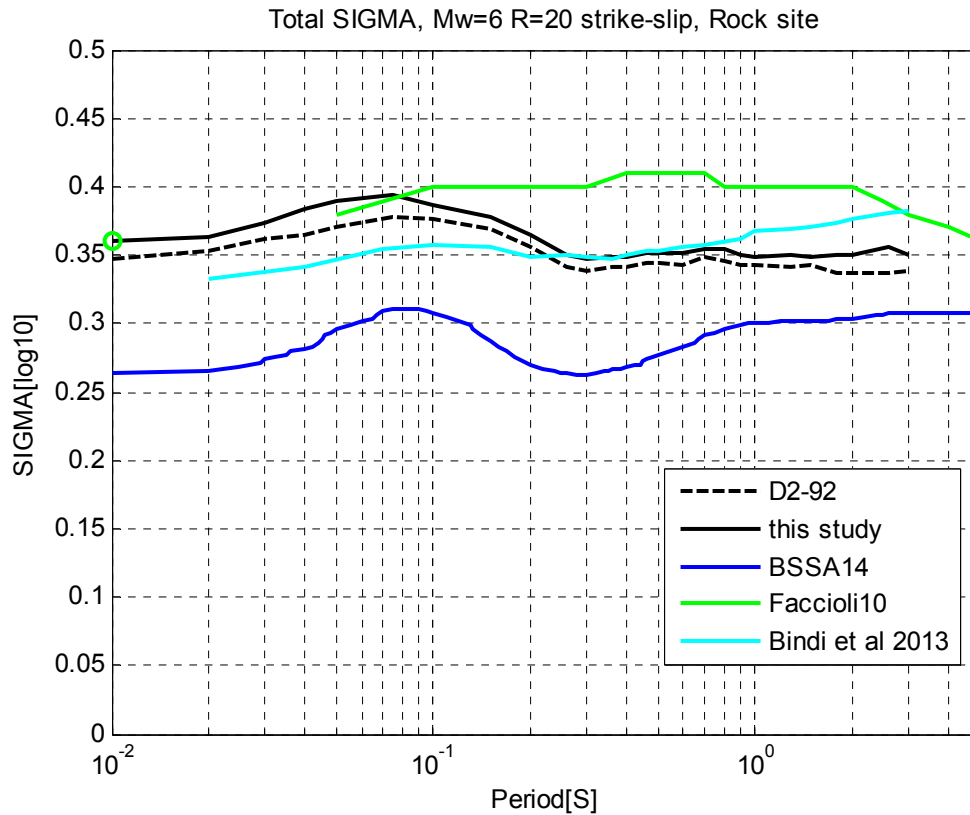


Figure 24: Total standard deviation (sigma) for the GMPEs considered in this section for comparison (see text for explanation). For the BSSA14 model, the sigma is computed for a Mw=6 and Rjb=20 km.

---

## 6. CONCLUSION

---

In this study we used the RESORCE-2013 database to derive an empirical GMPEs covering the magnitude range Mw=3-7.6 and for distances smaller than 200km. We first discussed the data selection and the metadata for French events. Then we introduced the generic functional form and discussed the results in terms of residuals. We carefully analyzed the residuals as a function of stress parameters available in literature for France and Switzerland. Finally we introduced the stress parameter scaling in the functional form. This allows to consider regional difference in the values of the stress parameter directly in the GMPE. The analysis of the residuals versus stress parameter highlighted some important results:

- the between-event residuals show a positive correlation with stress parameter;
- the slope of such correlation is very similar across different regions, the difference between regions is mostly related to the average stress parameter value;
- the scaling of the between-event residuals with stress parameter is in full agreement with what expected from the omega-square point-source model for similar magnitudes.



- the Mw and stress parameter values for the Pyrenees may be biased due to trade-off between source and attenuation parameters in the inversion by Drouet et al., (2010).

This study showed that the stress parameter can be reliably included in the functional form of the GMPE. On the one hand, it allows to account for regional differences in stress parameter and , on the other hand, it allows to decrease the standard deviation of the GMPE by partially explaining the large between-event variability observed at high-frequency for small magnitude events.

We investigated the within-event residuals searching for regional dependencies of ground motion attenuation with distance, in particular for the French data. Recent studies within the framework of the NGA-West2 project have pointed out that the attenuation of ground motion with distance may show significant deviation for one region to another (see e.g., Boore et al., 2014). Such difference are normally ascribed to difference in the term accounting for the “anelastic attenuation” in the GMPEs (a term describing the linear decay of the log of ground motion). This term, usually starts to play a role at relatively large distances. In this study we limited the maximum distance to 200 km, mostly because for magnitude below 4 then quality of the records at larger distances start to be poor. In this distance range the data does not require a term accounting for anelastic attenuation in the functional form. By looking at the residuals we didn't find any evidence suggesting regional difference in the attenuation of ground motion with distance. The French data , as a whole, do not show any trend with distance. In the same way, residuals separated for French regions, although represented by a much smaller number of data , seem to reject the hypothesis of regional differences in the attenuation.

In the functional form, we used a site effects model based on EC8 classes. This is certainly a disadvantage of the model as it may limit its application in site-specific PSHA where a specific value of Vs30 is usually specified. However, this was the price to pay in order to include a relevant amount of French data. Initiatives are ongoing within the SIGMA project devoted to the characterization of a number of French station in terms of Vs30. This will be an important information that will allow to improve the model when available.

Concerning the application of the model presented in this study we suggest to replace equation (7) with the following one:

$$F_{stress}(\Delta\sigma, Mw) = \begin{cases} r_1 \log_{10} \left( \frac{\Delta\sigma}{\Delta\sigma_{REF}} \right) & \text{for } Mw < 5.0 \\ r_1 \log_{10} \left( \frac{\Delta\sigma}{\Delta\sigma_{REF}} \right) (6.0 - Mw) & \text{for } 5.0 \leq Mw \leq 6.0 \\ 0 & \text{for } Mw > 6.0 \end{cases} \quad (8)$$

This model is identical to equation (7) for Mw < 5 but for larger magnitudes we introduce a taper that force the stress parameter scaling to reduce to zero at Mw>6. This is done because the stress parameter scaling is derived from data in a restricted magnitude range and it should not be used to larger magnitudes. In particular, the scaling of ground motion with stress parameter is expected to be different at larger magnitudes.

Finally, we recall that in the derivation of the stress parameter model, we converted the values provided by Edwards & Fah (2013) for Switzerland in order to be used consistently with the values for France by Drouet et al., (2010). This

means that in the application of the model if one want to use the values of stress parameters for Switzerland provided by Edwards & Fah (2013), those value need to be multiplied by a factor of 4.55 before using them in equation 8.

---

## 7. REFERENCES

---

- Abrahamson N A, Youngs RR (1992). A stable algorithm for regression analyses using the random effects model. *Bulletin of the Seismological Society of America*, 82(1), 505–510.
- Akkar S, Bommer JJ (2010). Empirical equations for the prediction of PGA, PGV, and spectral accelerations in Europe, the Mediterranean region, and the middle east. *Seismological Research Letters*, 81(2), 195–206. doi: 10.1785/gssrl.81.2.195
- Akkar S, Sandikkaya MA, Şenyurt M, Azari SA, Ay BÖ (2014a) Reference Database for Seismic Ground-Motion in Europe (RESORCE). *Bulletin of Earthquake Engineering*, in Press
- Akkar S., M.A. Sandikkaya, and J.J. Bommer (2014b). Empirical Ground-Motion Models for Point- and Extended-Source Crustal Earthquake Scenarios in Europe and the Middle East. *Bulletin of Earthquake Engineering*, in Press
- Ameri (2013). Preliminary GMPEs based on RESORCE-2013: effect on data selection and metadata uncertainties. Deliverable D2-92. SIGMA Project.
- Baize S., Cushing E.M., Lemeille F. and H. Jomard (2013). Updated seismotectonic zoning scheme of Metropolitan France, with reference to geologic and seismotectonic data. *Bull. Soc. géol. France*, 2013, t. 184, no 3, pp. 225-259.
- Bindi D., Massa M., Luzi L., Ameri G., Pacor F.,Puglia R. and P. Augliera (2014) Pan-European Ground-Motion Prediction Equations for the Average Horizontal Component of PGA, PGV, and 5%-Damped PSA at Spectral Periods up to 3.0 s using the RESORCE dataset. *Bulletin of Earthquake Engineering*, in Press
- Bommer JJ and S.Akkar (2012) Consistent Source-to-Site Distance Metrics in Ground-Motion Prediction Equations and Seismic Source Models for PSHA, *Earthquake Spectra*, Volume 28, No. 1, 1–15
- Boore DM, Atkinson GM (2008). Ground-motion prediction equations for the average horizontal component of PGA, PGV, and 5%-damped PSA at spectral periods between 0.01 s and 10.0 s, *Earthquake Spectra* 24, 99–138.
- Boore, D.M., J.P. Stewart, E. Seyhan, and G.M. Atkinson (2014). NGA-West 2 equations for predicting PGA, PGV, and 5%-damped PSA for shallow crustal earthquakes, *Earthquake Spectra*, (in press).
- Cara, M., Schlupp, A. et C. Sira, 2007. Observations sismologiques : sismicité de la France en 2003, 2004, 2005, Bureau central sismologique français, ULP/EOST - CNRS/INSU, Strasbourg.
- Courboux F., C. Larroque, A. Deschamps, C. Kohrs-Sansorny, C. G´elis, J. L. Got, J. Charreau, J. F. Stéphan, N. Béthoux, J. Virieux, D. Brunel, C. Maron, A. M. Duval, J-L. Perez and P. Mondielli (2007) Seismic hazard on the French Riviera: observations, interpretations and simulations. *Geophys. J. Int.*, 170, 387–400
- Drouet S., Cotton F. and P. Guéguen (2010). Vs30,  $\kappa$ , regional attenuation and Mw from accelerograms: application to magnitude 3–5 French earthquakes, *Geophys. J. Int.* doi: 10.1111/j.1365-246X.2010.04626.x

- Edwards, B. and D. Fäh (2013). A Stochastic Ground-Motion Model for Switzerland, *Bulletin of the Seismological Society of America* 103 (1), 78-98, doi: 10.1785/0120110331.
- Faccioli E, Bianchini A, Villani M (2010) New ground motion prediction equations for  $t > 1$  s and their influence on seismic hazard assessment. In: *Proceedings of the University of Tokyo Symposium on Long- Period Ground Motion and Urban Disaster Mitigation*, March 17–18, Tokyo, Japan
- Goertz-Allmann B. P., and B. Edwards (2014) Constraints on crustal attenuation and three-dimensional spatial distribution of stress drop in Switzerland, *Geophys. J. Int.* 196 (1): 493-509
- Joyner, W. B. and B. M. Boore (1981). Peak horizontal acceleration and velocity from strong-motion records including records from the 1979 Imperial Valley, California, earthquake, *Bull. Seism. Soc. Am.* 71, 2011-2038.
- Rigo A. , Souriau A., Dubos N., Sylvander M. and C. Ponsolles (2005) Analysis of the seismicity in the central part of the Pyrenees (France), and tectonic implications. *Journal of Seismology*, 9: 211–222
- Scherbaum, F., Schmedes, J. and Cotton, F., 2004, On the conversion of source-to-site distance measures for extended earthquake source model, *Bull. Seism. Soc. Am.* 94, 1053–1059.
- Sylvander M., Souriau A., Rigo A., Tocheport A., J Toutain, C. Ponsolles and S. Benahmed (2008) The 2006 November,  $M_L = 5.0$  earthquake near Lourdes (France): new evidence for NS extension across the Pyrenees. *Geophys. J. Int.* (2008) 175, 649–664
- Thouvenot, F., Frechet, J., Jenatton, L. and Garmond, J.F., 2003. The Belledune border Fault: Identification of an active seismic strike-slip fault in the western Alps, *Geophys. J. Int.*, 155, 174–192.
- Youngs, R. R., N. Abrahamson, F. I. Makdisi, and K. Singh (1995). Magnitude-dependent variance of peak ground acceleration. *Bulletin of the Seismological Society of America* 85 (4), 1,161–1,176.